

Meshfree Methods

Antonio Huerta², Ted Belytschko¹, Sonia Fernández-Méndez², Timon Rabczuk¹

¹ *Department of Mechanical Engineering, Northwestern University, 2145 Sheridan Road, Evanston, IL 60208, USA.*

² *Laboratori de Càlcul Numèric, Universitat Politècnica de Catalunya, Jordi Girona 1, E-08034 Barcelona, Spain.*

ABSTRACT

Aim of the present chapter is to provide an in-depth presentation and survey of mesh-free particle methods. Several particle approximation are reviewed; the SPH method, corrected gradient methods and the Moving least squares (MLS) approximation. The discrete equations are derived from a collocation scheme or as Galerkin method. Special attention is paid to the treatment of essential boundary conditions. A brief review over radial basis functions is given because they play a significant role in mesh-free methods. Finally, different approaches for modelling discontinuities in mesh-free methods are described.

KEY WORDS: Meshless, moving least squares, smooth particle hydrodynamics, element-free Galerkin, reproducing kernel particle methods, partitions of unity, radial basis, discontinuities, coupling with finite elements, incompressibility.

1. INTRODUCTION

As the range of phenomena that need to be simulated in engineering practice broadens, the limitations of conventional computational methods, such as finite elements, finite volumes or finite difference methods, have become apparent. There are many problems of industrial and academic interest which cannot be easily treated with these classical mesh-based methods: for example, the simulation of manufacturing processes such as extrusion and molding, where it is necessary to deal with extremely large deformations of the mesh, or simulations of failure, where the simulation of the propagation of cracks with arbitrary and complex paths is needed.

The underlying structure of the classical mesh-based methods is not well suited to the treatment of discontinuities that do not coincide with the original mesh edges. With a mesh-based method, the most viable strategy for dealing with moving discontinuities is to remesh whenever it is necessary. The remeshing process is costly and not trivial in 3D (if reasonable meshes are desired), and projection of quantities of interest between successive meshes usually leads to degradation of accuracy and often results in an excessive computational cost. Although some recent developments (Moes *et al.*, 1999, Wells *et al.*, 2002) partially overcome these difficulties, it is difficult to eliminate sensitivity to the choice of mesh.

The objective of mesh-free methods is to eliminate at least part of this mesh dependence by constructing the approximation entirely in terms of nodes (usually called particles in the

context of mesh-free methods). Moving discontinuities or interfaces can usually be treated without remeshing with minor costs and accuracy degradation (see, for instance, Belytschko and Organ, 1997). Thus the range of problems that can be addressed by mesh-free methods is much wider than mesh-based methods. Moreover, large deformations can be handled more robustly with mesh-free methods because the approximation is not based on elements whose distortion may degrade the accuracy. This is useful in both fluid and solid computations.

Another major drawback of mesh-based methods is the difficulty in ensuring for any real geometry a smooth, painless and seamless integration with Computer Aided Engineering (CAE), industrial Computer Aided Design (CAD) and Computer Aided Manufacturing (CAM) tools. Mesh-free methods have the potential to circumvent these difficulties. The elimination of mesh generation is the key issue. The advantages of mesh-free methods for 3D computations become particularly apparent.

Mesh-free methods also present obvious advantages in adaptive processes. There are *a priori* error estimates for most of the mesh-free methods. This allows the definition of adaptive refinement processes as in finite element computations: an *a posteriori* error estimate is computed and the solution is improved by adding nodes/particles where needed or increasing the order of the approximation until the error becomes acceptable, see e.g. Babuška and Melenk, 1995; Melenk and Babuška, 1996; Duarte and Oden, 1996b.

Mesh-free methods were originated over twenty-five years ago but it is in recent years that they have received substantial attention.

The approach that seems to have the longest continuous history is the *smooth particle hydrodynamic* (SPH) method by Lucy (1977) and Gingold and Monaghan (1977), see Section 2.1. It was first developed for modelling astrophysical phenomena without boundaries, such as exploding stars and dust clouds. Compared to other numerical methods, the rate of publications in this field was very modest for many years; progress is reflected in the review papers by Monaghan (1982; 1988).

Recently, there has been substantial improvement in these methods. For instance, Dyka (1994) and Sweegle *et al.* (1995) study its instabilities; Johnson and Beissel (1996) proposed a method for improving strain calculations; and Liu *et al.* (1995a) present a correction function for kernels in both the discrete and continuous case.

In fact, this approach can be seen as a variant of *moving least-squares* (MLS) approximations (see Section 2.2). A detailed description of MLS approximants can be found in Lancaster (1981). Nayroles *et al.* (1992) were evidently the first to use moving least square approximations in a Galerkin weak form and called it the *diffuse element method* (DEM). Belytschko *et al.* (1994) refined the method and extended it to discontinuous approximations and called it *element-free Galerkin* (EFG). Duarte and Oden (1996a) and Babuška and Melenk (1995) recognize that the methods are specific instances of *partitions of unity* (PU). These authors and Liu *et al.* (1997a) were also among the first to prove convergence of this class of methods.

This class of methods (EFG, DEM, PU, among others) is consistent and, in the forms proposed stable, although substantially more expensive than SPH, because of the need of a very accurate integration. Zhu and Atluri (1998) propose a Petrov-Galerkin weak form in order to facilitate the computation of the integrals, but usually leading to non symmetric systems of equations. De and Bathe (2000) use this approach for a particular choice of the approximation space and the Petrov-Galerkin weak form and call it the *method of finite spheres*.

On a parallel path, Vila (1999) has introduced a different mesh-free approximation specially suited for conservation laws: the *renormalized meshless derivative* (RMD) with turns out to

give accurate approximation of derivatives in the framework of collocation approaches. Two other paths in the evolution of mesh-free methods have been the development of generalized finite difference methods, which can deal with arbitrary arrangements of nodes, and particle-in-cell methods. One of the early contributors to the former was Perrone and Kao (1975), but Liszka and Orkisz (1980) proposed a more robust method. Recently these methods have taken a character which closely resembles the moving least squares methods and partitions of unity.

In recent papers the possibilities of mesh-free methods have become apparent. The special issue (Liu *et al.*, 1996a) shows the ability of mesh-free methods to handle complex simulations, such as impact, cracking or fluid dynamics. Bouillard and Suleau (1998) apply a mesh-free formulation to acoustic problems with good results. Bonet and Lok (1999) introduce a gradient correction in order to preserve the linear and angular momentum with applications to fluid dynamics. Bonet and Kulasegaram (2000) proposes the introduction of integration correction that improves accuracy with applications to metal forming simulation. Oñate and Idelsohn (1998) propose a mesh-free method, the *finite point method*, based on a weighted least-squares approximation with point collocation with applications to convective transport and fluid flow. Recently several authors have proposed mixed approximations combining finite elements and mesh-free methods, in order to exploit of the advantages of each method (see Belytschko *et al.*, 1995; Hegen, 1996; Liu *et al.*, 1997b; Huerta and Fernández-Méndez, 2000).

Several review papers and books have been published on mesh-free methods; Belytschko *et al.* (1996a), Li and Liu (2002) and Liu *et al.* (1995b). This chapter will build on Belytschko *et al.* (1996a) and give a different perspective from the others.

2. APPROXIMATION IN MESH-FREE METHODS

This section describes the most common approximants in mesh-free methods. We will employ the name “approximants” rather than interpolants that is often mistakenly used in the mesh-free literature because as shown later, these approximants usually do not pass through the data, so they are not interpolants. Meshfree approximants can be classified in two families: those based on *smooth particle hydrodynamics* (SPH) and those based on *moving least-squares* (MLS). As will be noted in Section 3 the SPH approximants are usually combined with collocation or point integration techniques, while the MLS approximants are customarily applied with Galerkin formulations, though collocation techniques are growing in popularity.

2.1. Smooth particle hydrodynamic

2.1.1. The early SPH The earliest mesh-free method is the SPH method, Lucy (1977). The basic idea is to approximate a function $u(x)$ by a convolution

$$u(\mathbf{x}) \simeq \tilde{u}^\rho(\mathbf{x}) := \int C_\rho \phi\left(\frac{\mathbf{y} - \mathbf{x}}{\rho}\right) u(\mathbf{y}) \, d\mathbf{y}, \quad (1)$$

where ϕ is a compactly supported function, usually called a *window function* or *weight function*, and ρ is the so-called dilation parameter. The support of the function is sometimes called the domain of influence. The dilation parameter characterizes the size of the support of $\phi(\mathbf{x}/\rho)$, usually by its radius. C_ρ is a normalization constant such that

$$\int C_\rho \phi\left(\frac{\mathbf{y}}{\rho}\right) \, d\mathbf{y} = 1. \quad (2)$$

One way to develop a discrete approximation from (1) is to use numerical quadrature

$$u(\mathbf{x}) \simeq \tilde{u}^\rho(\mathbf{x}) \simeq u^\rho(\mathbf{x}) := \sum_I C_\rho \phi\left(\frac{\mathbf{x}_I - \mathbf{x}}{\rho}\right) u(\mathbf{x}_I) \omega_I$$

where \mathbf{x}_I and ω_I are the points and weights of the numerical quadrature. The quadrature points are usually called *particles*. The previous equation can also be written as

$$u(\mathbf{x}) \simeq \tilde{u}^\rho(\mathbf{x}) \simeq u^\rho(\mathbf{x}) := \sum_I \omega(\mathbf{x}_I, \mathbf{x}) u(\mathbf{x}_I), \quad (3)$$

where the discrete window function is defined as

$$\omega(\mathbf{x}_I, \mathbf{x}) = C_\rho \phi\left(\frac{\mathbf{x}_I - \mathbf{x}}{\rho}\right).$$

Thus, the SPH mesh-free approximation can be defined as

$$u(\mathbf{x}) \simeq u^\rho(\mathbf{x}) = \sum_I N_I(\mathbf{x}) u(\mathbf{x}_I),$$

with the approximation basis $N_I(\mathbf{x}) = \omega(\mathbf{x}_I, \mathbf{x})$.

Remark 1. Note that, in general, $u^\rho(\mathbf{x}_I) \neq u(\mathbf{x}_I)$. That is, the shape functions are not interpolants, i.e. they do not verify the Kronecker delta property:

$$N_J(\mathbf{x}_I) \neq \delta_{IJ}.$$

This is common for all particle methods (see Figure 5 for the MLS approximant) and thus special techniques are needed to impose essential boundary conditions (see Section 3).

Remark 2. The dilation parameter ρ characterizes the support of the approximants $N_I(\mathbf{x})$.

Remark 3. In contrast to finite elements, the neighbor particles (particles belonging to a given support) have to be identified during the course of the computation. This is of special importance if the domain of support changes in time and requires fast neighbor search algorithms, a crucial feature for the effectiveness of a mesh-free method, see e.g. Schweitzer (2003).

Remark 4. There is an optimal value for the ratio between the dilation parameter ρ and the distance between particles h . Figure 1 shows that for a fixed distribution of particles, h constant, the dilation parameter must be large enough to avoid aliasing (spurious short waves in the approximated solution). It also shows that an excessively large value for ρ will lead to excessive smoothing. For this reason, it is usual to maintain a constant ratio between the dilation parameter ρ and the distance between particles h .

2.1.2. Window functions The window function plays an important role in mesh-free methods. Other names for the window function are kernel and weight function. The window function may be defined in various manners. For 1D the most common choices are
Cubic spline:

$$\phi_{1D}(x) = 2 \begin{cases} 4(|x| - 1)x^2 + 2/3 & |x| \leq 0.5 \\ 4(1 - |x|)^3/3 & 0.5 \leq |x| \leq 1 \\ 0 & 1 \leq |x|, \end{cases} \quad (4)$$

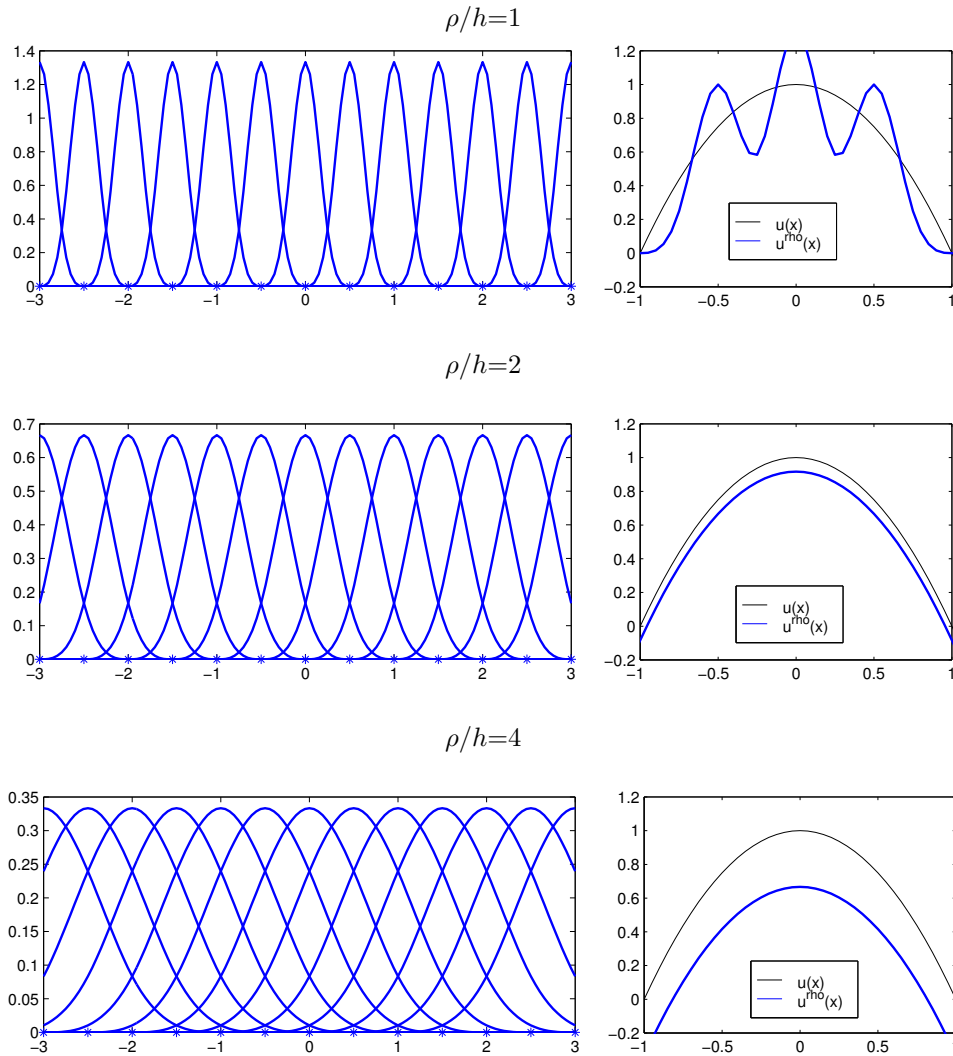


Figure 1. SPH approximation functions and approximation of $u(x) = 1 - x^2$ with cubic spline window function, distance between particles $h = 0.5$ and quadrature weights $\omega_i = h$, for $\rho/h = 1, 2, 4$.

Gaussian:

$$\phi_{1D}(x) = \begin{cases} (\exp(-9x^2) - \exp(-9))/(1 - \exp(-9)) & |x| \leq 1 \\ 0 & 1 \leq |x|. \end{cases} \quad (5)$$

The above window function can easily be extended to higher dimensions. For example, in 2D the most common extensions are

Radial basis function:

$$\phi(\mathbf{x}) = \phi_{1D}(\|\mathbf{x}\|),$$

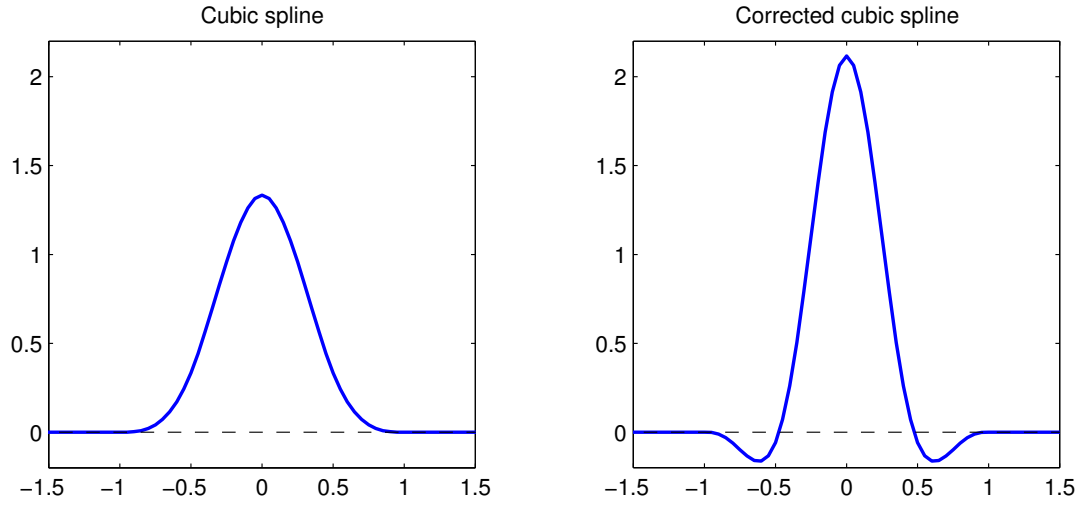


Figure 2. Cubic spline and corrected window function for polynomials of degree 2.

Rectangular supported window function:

$$\phi(\mathbf{x}) = \phi_{1D}(|x_1|) \phi_{1D}(|x_2|)$$

where, as usual, $\mathbf{x} = (x_1, x_2)$ and $\|\mathbf{x}\| = \sqrt{x_1^2 + x_2^2}$.

2.1.3. Design of window functions In the continuous SPH approximation (1), a window function ϕ can easily be modified to exactly reproduce a polynomial space \mathcal{P}_m in \mathbb{R} of degree $\leq m$, i.e.

$$p(x) = \int C_\rho \phi\left(\frac{y-x}{\rho}\right) p(y) dy, \quad \forall p \in \mathcal{P}_m. \quad (6)$$

If the following conditions are satisfied

$$\int C_\rho \phi\left(\frac{y}{\rho}\right) dy = 1, \quad \int C_\rho \phi\left(\frac{y}{\rho}\right) y^j dy = 0 \text{ for } 0 < j \leq m$$

the window function is able to reproduce the polynomial space \mathcal{P}_m . Note that the first condition coincides with (2) and defines the normalization constant, i.e. it imposes the reproducibility of constant functions. These equations are often referred as *consistency conditions* although, a more appropriate term would be completeness conditions.

For example, the window function

$$\tilde{\phi}(x) = \left(\frac{27}{17} - \frac{120}{17} x^2 \right) \phi(x), \quad (7)$$

where $\phi(x)$ is the cubic spline, reproduces the second degree polynomial basis $\{1, x, x^2\}$. Figure 2 shows the cubic spline defined in (4) and the corrected window function (7), see Liu *et al.* (1996b) for details.

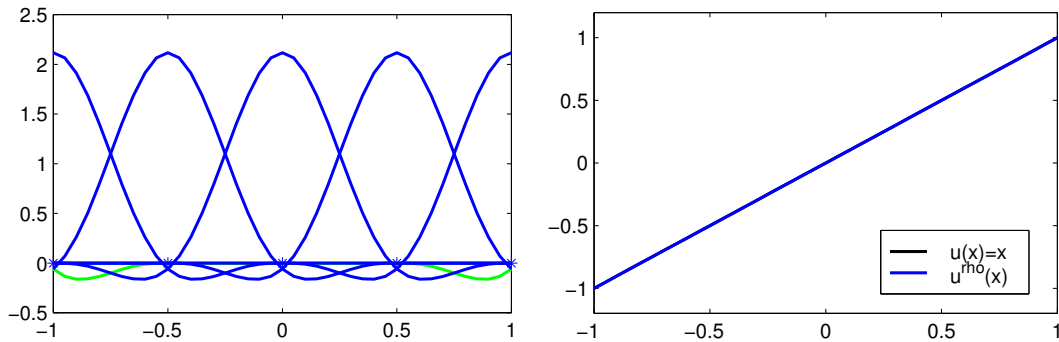


Figure 3. Modified cubic splines and particles, $h = 0.5$, and SPH discrete approximation for $u(x) = x$ with $\rho/h = 2$ in an “unbounded domain”.

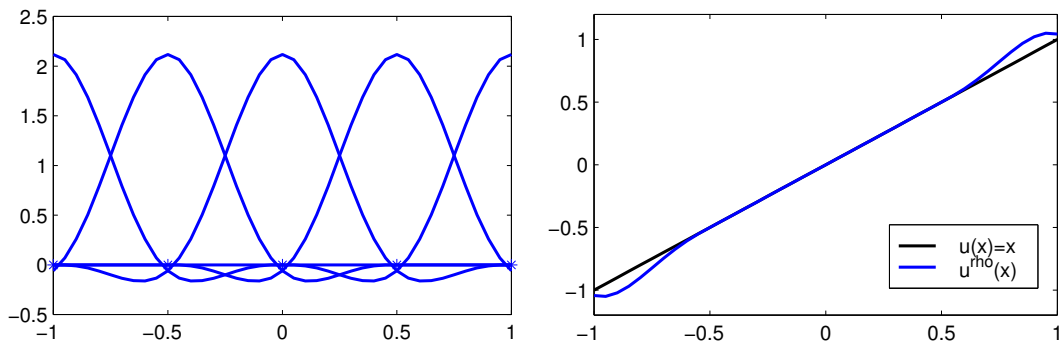


Figure 4. Modified cubic splines and particles, $h = 0.5$, and SPH discrete approximation for $u(x) = x$ with $\rho/h = 2$ in a bounded domain.

However, the design of the window function is not trivial in the presence of boundaries or with nonuniform distributions of particles (see Section 2.2). Figure 3 shows the corrected cubic spline window functions associated with a uniform distribution of particles, with distance $h = 0.5$ between particles and $\rho = 2h$, and the discrete SPH approximation described by (3) for $u(x) = x$ with uniform weights $\omega_I = h$. The particles outside the interval $[-1, 1]$ are considered in the approximation, as in an unbounded domain (the corresponding translated window functions are depicted with green). The linear monomial $u(x) = x$ is exactly reproduced. However, in a bounded domain, the approximation is not exact near the boundaries when only the particles in the domain, $[-1, 1]$ are considered in this example, see Figure 4.

Remark 5 (Consistency) *If the approximation reproduces exactly a basis of the polynomials of degree less or equal to m then the approximation is said to have m -order consistency.*

2.1.4. Correcting the SPH method The SPH approximation is used in the solution of PDEs, usually through a collocation technique or point integration approaches, see Monaghan (1982),

Vila (1999), Bonet and Lok (1999) and Section 3.1. Thus, it is necessary to compute accurate approximations of the derivatives of the dependent variables. The derivatives provided by original SPH method can be quite inaccurate, and thus, it is necessary to improve the approximation, or its derivatives, in some manner.

Randles and Libersky (1996), Krongauz and Belytschko (1998a) and Vila (1999) proposed a correction of the gradient: the *renormalized meshless derivative* (RMD). It is an extension of the partial correction proposed by Johnson and Beissel (1996). Let the derivatives of a function u be approximated as the derivatives of the SPH approximation defined in (3),

$$\nabla u(\mathbf{x}) \simeq \nabla u^\rho(\mathbf{x}) = \sum_I \nabla \omega(\mathbf{x}_I, \mathbf{x}) u(\mathbf{x}_I).$$

The basic idea of the RMD approximation is to define a corrected derivative

$$D^\rho u(\mathbf{x}) := \sum_J \mathbf{B}(\mathbf{x}) \nabla \omega(\mathbf{x}_J, \mathbf{x}) u(\mathbf{x}_J), \quad (8)$$

where the correction matrix $\mathbf{B}(\mathbf{x})$ is chosen such that $\nabla u(\mathbf{x}) = D^\rho u(\mathbf{x})$ for all linear polynomials. In Vila (1999), a symmetrized approximation for the derivatives is defined

$$D_S^\rho u(\mathbf{x}) := D^\rho u(\mathbf{x}) - D^\rho 1(\mathbf{x}) u(\mathbf{x}), \quad (9)$$

where, by definition (8),

$$D^\rho 1(\mathbf{x}) = \sum_J \mathbf{B}(\mathbf{x}) \nabla \omega(\mathbf{x}_J, \mathbf{x}),$$

Note that (9) interpolates exactly the derivatives when $u(\mathbf{x})$ is constant. The consistency condition $\nabla u(\mathbf{x}) = D_S^\rho u(\mathbf{x})$ must be imposed only for linear monomials

$$\mathbf{B}(\mathbf{x}) = \left[\sum_J \nabla \omega(\mathbf{x}_J, \mathbf{x}) (\mathbf{x}_J - \mathbf{x})^\top \right]^{-1}.$$

If the ratio between the dilation parameter ρ and the distance between particles remains constant, there are *a priori* error bounds for the RMD, $D_S^\rho u$, similar to the linear finite element ones, where ρ plays the role of the element size in finite elements, Vila (1999).

In SPH, the interparticle forces coincide with the vector joining them, so conservation of linear and angular momentum are met for each point pair. In other words, linear and angular momentum are conserved locally, see Dilts (1999).

When the kernels are corrected to reproduce linear polynomials or the derivatives of linear polynomials, these local conservation properties are lost. However, global linear and translational momentum are conserved if the approximation reproduces linear functions, see Krongauz and Belytschko (1998a) and Bonet and Lok (1999).

Although the capability to reproduce a polynomial of a certain order is an ingredient in many convergence proofs of solutions for PDEs, it does not suffice to pass the patch test. Krongauz and Belytschko (1998b) found that corrected gradient methods do not satisfy the patch test and exhibit poor convergence when the corrected gradient is used for the test function. They showed that a Petrov-Galerkin method with Shepard test functions satisfies the patch test.

There are other ways of correcting the SPH method. For example, Bonet and Lok (1999) combine a correction of the window function, as in the RKPM method (see Section 2.2),

and a correction of the gradient to preserve angular momentum. In fact, there are a lot of similarities between the corrected SPH and the renormalized meshless derivative. The most important difference between the RMD approach where the 0-order consistency is obtained by the definition of the symmetrized gradient (8), and the corrected gradient $\tilde{\nabla}u^\rho$ is that in this case 0-order consistency is obtained with the Shepard function.

With a similar rationale, Bonet and Kulasegaram (2000) present a correction of the window function and an integration corrected vector for the gradients (in the context of metal forming simulations). The corrected approximation is used in a weak form with numerical integration at the particles (see Section 3.2). Thus, the gradient must be evaluated only at the particles. However, usually the particle integration is not accurate enough and the approximation fails to pass the patch test. In order to obtain a consistent approximation a corrected gradient is defined. At every particle \mathbf{x}_I the corrected gradient is computed as

$$\tilde{\nabla}u^\rho(\mathbf{x}_I) = \nabla u^\rho(\mathbf{x}_I) + \boldsymbol{\gamma}_I \llbracket u \rrbracket_I$$

where $\boldsymbol{\gamma}_I$ is the correction vector (one component for each spatial dimension) at particle \mathbf{x}_I and where the bracket $\llbracket u \rrbracket_I$ is defined as $\llbracket u \rrbracket_I = u(\mathbf{x}_I) - u^\rho(\mathbf{x}_I)$. These extra parameters, $\boldsymbol{\gamma}_I$, are determined requiring that the patch test be passed. A global linear system of equations must be solved to compute the correction vector and to define the derivatives of the approximation; then, the approximation of u and its derivatives are used to solve the boundary value problem.

2.2. Moving least-squares interpolants

2.2.1. Continuous moving least-squares The objective of the MLS approach is to obtain an approximation similar to the SPH one (1), with high accuracy even in a bounded domain. Let us consider a bounded, or unbounded, domain Ω . The basic idea of the MLS approach is to approximate $u(\mathbf{x})$, at a given point \mathbf{x} , through a polynomial least-squares fit of u in a neighborhood of \mathbf{x} . That is, for fixed $\mathbf{x} \in \Omega$, and \mathbf{z} near \mathbf{x} , $u(\mathbf{z})$ is approximated with a polynomial expression

$$u(\mathbf{z}) \simeq \tilde{u}^\rho(\mathbf{z}, \mathbf{x}) = \mathbf{P}^\top(\mathbf{z}) \mathbf{c}(\mathbf{x}) \quad (10)$$

where the coefficients $\mathbf{c}(\mathbf{x}) = \{c_0(\mathbf{x}), c_1(\mathbf{x}), \dots, c_l(\mathbf{x})\}^\top$ are not constant, they depend on point \mathbf{x} , and $\mathbf{P}(\mathbf{z}) = \{p_0(\mathbf{z}), p_1(\mathbf{z}), \dots, p_l(\mathbf{z})\}^\top$ includes a complete basis of the subspace of polynomials of degree m . It can also include exact features of a solution, such as cracktip fields, as described in Ventura *et al.* (2002). The vector $\mathbf{c}(\mathbf{x})$ is obtained by a least-squares fit, with the scalar product

$$\langle f, g \rangle_{\mathbf{x}} = \int_{\Omega} \phi\left(\frac{\mathbf{y} - \mathbf{x}}{\rho}\right) f(\mathbf{y}) g(\mathbf{y}) \, d\mathbf{y}. \quad (11)$$

That is, the coefficients \mathbf{c} are obtained by minimization of the functional $\tilde{J}_{\mathbf{x}}(\mathbf{c})$ centered in \mathbf{x} and defined by

$$\tilde{J}_{\mathbf{x}}(\mathbf{c}) = \int_{\Omega} \phi\left(\frac{\mathbf{y} - \mathbf{x}}{\rho}\right) [u(\mathbf{y}) - \mathbf{P}(\mathbf{y}) \mathbf{c}(\mathbf{x})]^2 \, d\mathbf{y}, \quad (12)$$

where $\phi((\mathbf{y} - \mathbf{x})/\rho)$ is the compact supported weighting function. The same weighting/window functions as for SPH, given in Section 2.1.2, are used.

Remark 6. *Thus, the scalar product is centered at the point \mathbf{x} and scaled with the dilation parameter ρ . In fact, the integration is constructed in a neighborhood of radius ρ centered at \mathbf{x} , that is, in the support of $\phi((\cdot - \mathbf{x})/\rho)$.*

Remark 7 (Polynomial space) *In one dimension, we can let $p_i(x)$ be the monomials x^i , and, in this particular case, $l = m$. For larger spatial dimensions two types of polynomial spaces are usually chosen: the set of polynomials, \mathcal{P}_m , of total degree $\leq m$, and the set of polynomials, \mathcal{Q}_m , of degree $\leq m$ in each variable. Both include a complete basis of the subspace of polynomials of degree m . This, in fact, characterizes the a priori convergence rate, see Liu et al. (1997a) or Fernández-Méndez et al. (2003).*

The vector $\mathbf{c}(\mathbf{x})$ is the solution of the *normal equations*, that is, the linear system of equations

$$\mathbf{M}(\mathbf{x}) \mathbf{c}(\mathbf{x}) = \langle \mathbf{P}, u \rangle_{\mathbf{x}} \quad (13)$$

where $\mathbf{M}(\mathbf{x})$ is the Gram matrix (sometimes called a moment matrix) ,

$$\mathbf{M}(\mathbf{x}) = \int_{\Omega} \phi\left(\frac{\mathbf{y} - \mathbf{x}}{\rho}\right) \mathbf{P}(\mathbf{y}) \mathbf{P}^T(\mathbf{y}) \, d\mathbf{y}. \quad (14)$$

From (14) and (10), the least-squares approximation of u in a neighborhood of \mathbf{x} is:

$$u(\mathbf{z}) \simeq \tilde{u}^{\rho}(\mathbf{z}, \mathbf{x}) = \mathbf{P}^T(\mathbf{z}) \mathbf{M}^{-1}(\mathbf{x}) \langle \mathbf{P}, u \rangle_{\mathbf{x}}. \quad (15)$$

Since the weighting function ϕ usually favors the central point \mathbf{x} , it seems reasonable to assume that such an approximation is more accurate precisely at $\mathbf{z} = \mathbf{x}$ and thus the approximation (15) is particularized at \mathbf{x} , that is,

$$u(\mathbf{x}) \simeq \tilde{u}^{\rho}(\mathbf{x}) := \tilde{u}^{\rho}(\mathbf{x}, \mathbf{x}) = \int_{\Omega} \phi\left(\frac{\mathbf{y} - \mathbf{x}}{\rho}\right) \mathbf{P}^T(\mathbf{x}) \mathbf{M}^{-1}(\mathbf{x}) \mathbf{P}(\mathbf{y}) u(\mathbf{y}) \, d\mathbf{y}, \quad (16)$$

where the definition of the scalar product, equation (11), has been explicitly used. Equation (16) can be rewritten as

$$u(\mathbf{x}) \simeq \tilde{u}^{\rho}(\mathbf{x}) = \int_{\Omega} C_{\rho}(\mathbf{y}, \mathbf{x}) \phi\left(\frac{\mathbf{y} - \mathbf{x}}{\rho}\right) u(\mathbf{y}) \, d\mathbf{y},$$

which is similar to the SPH approximation, see equation (1), and with the scalar correction term $C_{\rho}(\mathbf{y}, \mathbf{x})$ defined as

$$C_{\rho}(\mathbf{y}, \mathbf{x}) := \mathbf{P}^T(\mathbf{x}) \mathbf{M}^{-1}(\mathbf{x}) \mathbf{P}(\mathbf{y}).$$

The function defined by the product of the correction and the window function ϕ ,

$$\Phi(\mathbf{y}, \mathbf{x}) := C_{\rho}(\mathbf{y}, \mathbf{x}) \phi\left(\frac{\mathbf{y} - \mathbf{x}}{\rho}\right),$$

is usually called *kernel function*. The new correction term depends on the point \mathbf{x} and the integration variable \mathbf{y} ; it provides an accurate approximation even in the presence of boundaries, see Liu et al. (1996b) for more details. In fact, the approximation verifies the following consistency property, see also Wendland (2001).

Proposition 1 (Consistency/reproducibility property) *The MLS approximation exactly reproduces all the polynomials in \mathbf{P} .*

Proof. The MLS approximation of the polynomials $p_i(\mathbf{x})$ is

$$\tilde{p}_i^{\rho}(\mathbf{x}) = \mathbf{P}^T(\mathbf{x}) \mathbf{M}^{-1}(\mathbf{x}) \langle \mathbf{P}, p_i \rangle_{\mathbf{x}} \quad \text{for } i = 0, \dots, l,$$

or, equivalently, in vector form

$$[\tilde{\mathbf{P}}^\rho]^\top(\mathbf{x}) = \mathbf{P}^\top(\mathbf{x}) \mathbf{M}^{-1}(\mathbf{x}) \underbrace{\int_{\Omega} \phi\left(\frac{\mathbf{y}-\mathbf{x}}{\rho}\right) \mathbf{P}(\mathbf{y}) \mathbf{P}^\top(\mathbf{y}) \, d\mathbf{y}}_{\mathbf{M}(\mathbf{x})}.$$

Therefore, using the definition of \mathbf{M} , see (14), it is trivial to verify that $\tilde{\mathbf{P}}^\rho(\mathbf{x}) \equiv \mathbf{P}(\mathbf{x})$. \square

2.2.2. Reproducing kernel particle method approximation Application of a numerical quadrature in (16) leads to the *reproducing kernel particle method* (RKPM) approximation

$$u(\mathbf{x}) \simeq \tilde{u}^\rho(\mathbf{x}) \simeq u^\rho(\mathbf{x}) := \sum_{I \in S_x^\rho} \omega(\mathbf{x}_I, \mathbf{x}) \mathbf{P}^\top(\mathbf{x}) \mathbf{M}^{-1}(\mathbf{x}) \mathbf{P}(\mathbf{x}_I) u(\mathbf{x}_I),$$

where $\omega(\mathbf{x}_I, \mathbf{x}) = \omega_I \phi((\mathbf{x}_I - \mathbf{x})/\rho)$ and \mathbf{x}_I and ω_I are integration points (particles) and weights, respectively. The particles cover the computational domain Ω , $\Omega \subset \mathbb{R}^{\text{nsd}}$. Let S_x^ρ be the index set of particles whose support include the point \mathbf{x} , see Remark 9. This approximation can be written as

$$u(\mathbf{x}) \simeq u^\rho(\mathbf{x}) = \sum_{I \in S_x} N_I(\mathbf{x}) u(\mathbf{x}_I) \quad (17)$$

where the approximation functions are defined by

$$N_I(\mathbf{x}) = \omega(\mathbf{x}_I, \mathbf{x}) \mathbf{P}^\top(\mathbf{x}) \mathbf{M}^{-1}(\mathbf{x}) \mathbf{P}(\mathbf{x}_I). \quad (18)$$

Remark 8. *In order to preserve the consistency/reproducibility property, the matrix \mathbf{M} , defined in (14), must be evaluated with the same quadrature used in the discretization of (16), see Chen et al. (1996) for details. That is, matrix $\mathbf{M}(\mathbf{x})$ must be computed as*

$$\mathbf{M}(\mathbf{x}) = \sum_{I \in S_x^\rho} \omega(\mathbf{x}_I, \mathbf{x}) \mathbf{P}(\mathbf{x}_I) \mathbf{P}^\top(\mathbf{x}_I). \quad (19)$$

Remark 9. *The sums in (17) and (19) only involve the indices I such that $\phi(\mathbf{x}_I, \mathbf{x}) \neq 0$, that is, particles \mathbf{x}_I in a neighborhood of \mathbf{x} . Thus, the set of neighboring particles is defined by the set of indices*

$$S_x^\rho := \{J \text{ such that } \|\mathbf{x}_J - \mathbf{x}\| \leq \rho\}.$$

Remark 10 (Conditions on particle distribution) *The matrix $\mathbf{M}(\mathbf{x})$ in (19) must be regular at every point \mathbf{x} in the domain. Liu et al. (1997a) discuss the necessary conditions. In fact, this matrix can be viewed, see Huerta and Fernández-Méndez (2000) or Fernández-Méndez and Huerta (2002), as a Gram matrix defined with a discrete scalar product*

$$\langle f, g \rangle_{\mathbf{x}} = \sum_{I \in S_x^\rho} \omega(\mathbf{x}_I, \mathbf{x}) f(\mathbf{x}_I) g(\mathbf{x}_I). \quad (20)$$

If this scalar product is degenerated, $\mathbf{M}(\mathbf{x})$ is singular. Regularity of $\mathbf{M}(\mathbf{x})$ is ensured by having enough particles in the neighborhood of every point x and avoiding degenerate patterns, that is

- (i) $\text{card } S_x^\rho \geq l + 1$.
- (ii) $\nexists F \in \text{span}\{p_0, p_1, \dots, p_l\} \setminus \{0\}$ such that $F(\mathbf{x}_I) = 0 \forall I \in S_x^\rho$.

Condition (ii) is easily verified. For instance, for $m = 1$ (linear interpolation) the particles cannot lie in the same straight line or plane for, respectively, 2D and 3D. In 1D, for any value of m , it suffices that different particles do not have the same position. Under these conditions one can compute the vector $\mathbf{P}^T(\mathbf{x})\mathbf{M}^{-1}(\mathbf{x})$ at each point and thus determine, from (18), the shape functions, $N_I(\mathbf{x})$.

2.2.3. Discrete MLS: element-free Galerkin approximation The MLS development, already presented in Section 2.2.1 for the continuous case (i.e. using integrals), can be developed directly from a discrete formulation. As in the continuous case, the idea is to approximate $u(\mathbf{x})$, at a given point \mathbf{x} , by a polynomial least-squares fit of u in a neighborhood of \mathbf{x} . That is, the same expression presented in (10) can be used, namely for fixed $\mathbf{x} \in \Omega$, and \mathbf{z} near \mathbf{x} , $u(\mathbf{z})$ is approximated with the polynomial expression

$$u(\mathbf{z}) \simeq u^\rho(\mathbf{z}, \mathbf{x}) = \mathbf{P}^T(\mathbf{z}) \mathbf{c}(\mathbf{x}). \quad (21)$$

In the framework of the element-free Galerkin (EFG) method, the vector $\mathbf{c}(\mathbf{x})$ is also obtained by a least-squares fit, with the discrete scalar product defined in (20), where $\omega(\mathbf{x}_I, \mathbf{x})$ is the discrete weighting function, which is equivalent to the window function

$$\omega(\mathbf{x}_I, \mathbf{x}) = \phi\left(\frac{\mathbf{x}_I - \mathbf{x}}{\rho}\right), \quad (22)$$

and $S_{\mathbf{x}}^\rho$ is the set of indices of neighboring particles defined in Remark 9. That is, the coefficients \mathbf{c} are obtained by minimization of the discrete functional $J_{\mathbf{x}}(\mathbf{c})$ centered in \mathbf{x} and defined by

$$J_{\mathbf{x}}(\mathbf{c}) = \sum_{I \in S_{\mathbf{x}}^\rho} \omega(\mathbf{x}_I, \mathbf{x}) [u(\mathbf{x}_I) - \mathbf{P}(\mathbf{x}_I) \mathbf{c}(\mathbf{x})]^2. \quad (23)$$

The normal equations are defined in a similar manner,

$$\mathbf{M}(\mathbf{x}) \mathbf{c}(\mathbf{x}) = \langle \mathbf{P}, u \rangle_{\mathbf{x}}, \quad (24)$$

and the Gram matrix is directly obtained from the discrete scalar product, see equation (19). After substitution of the solution of (24) in (21), the least-squares approximation of u in a neighborhood of \mathbf{x} is obtained

$$u(\mathbf{z}) \simeq u^\rho(\mathbf{z}, \mathbf{x}) = \mathbf{P}^T(\mathbf{z}) \mathbf{M}^{-1}(\mathbf{x}) \sum_{I \in S_{\mathbf{x}}^\rho} \omega(\mathbf{x}_I, \mathbf{x}) \mathbf{P}(\mathbf{x}_I) u(\mathbf{x}_I). \quad (25)$$

Particularization of (25) at $\mathbf{z} = \mathbf{x}$ leads to the discrete MLS approximation of $u(\mathbf{x})$

$$u(\mathbf{x}) \simeq u^\rho(\mathbf{x}) := u^\rho(\mathbf{x}, \mathbf{x}) = \sum_{I \in S_{\mathbf{x}}^\rho} \omega(\mathbf{x}_I, \mathbf{x}) \mathbf{P}^T(\mathbf{x}) \mathbf{M}^{-1}(\mathbf{x}) \mathbf{P}(\mathbf{x}_I) u(\mathbf{x}_I). \quad (26)$$

This EFG approximation coincides with the RKPM one described in equations (18) and (19).

Remark 11 (Convergence) Liu et al. (1997a) showed convergence of the RKPM and EFG. The a priori error bound is very similar to the bound in finite elements. The parameter ρ plays the role of h , and m (the order of consistency) plays the role of the degree of the approximation polynomials in the finite element mesh. Convergence properties depend on m and ρ . They do not depend on the distance between particles because usually this distance is proportional to ρ , i.e. the ratio between the particle distance over the dilation parameter is of order one, see Liu et al. (1997a).

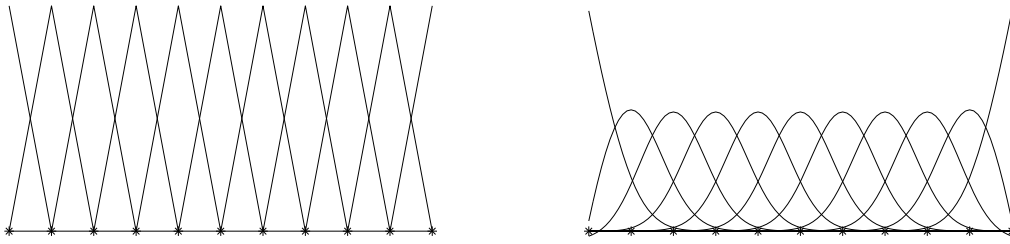


Figure 5. Interpolation functions with $\rho/h \simeq 1$ (similar to finite elements) and $\rho/h = 2.6$, with cubic spline and linear consistency.

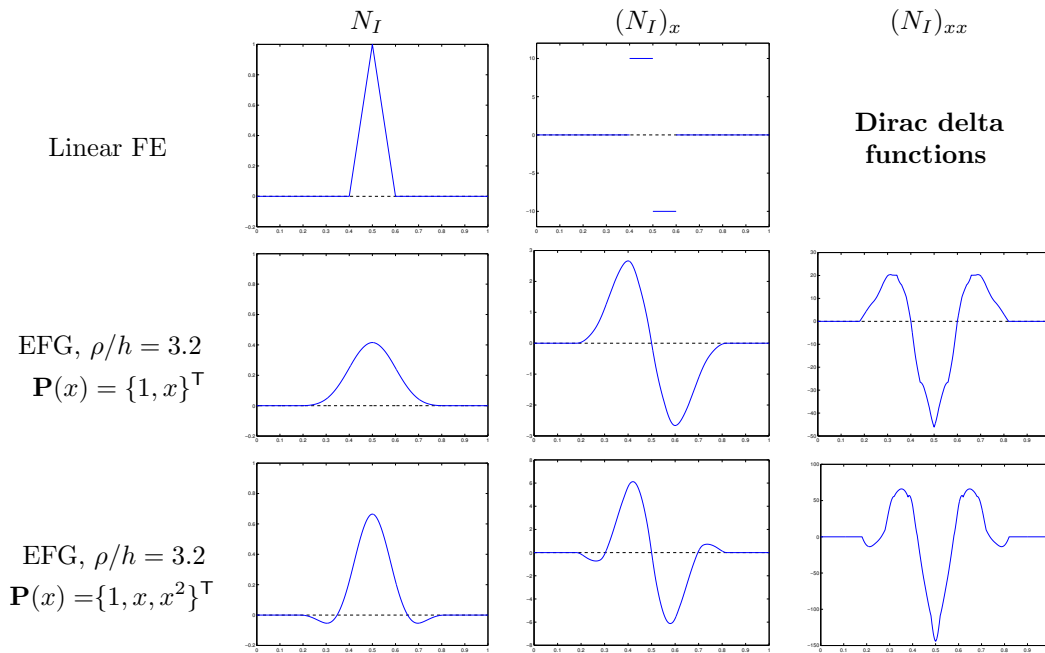


Figure 6. Shape function and derivatives for linear finite elements and the EFG approximation.

Remark 12. *The approximation is characterized by the order of consistency required, i.e. the complete basis of polynomials employed in \mathbf{P} , and by the ratio between the dilation parameter and the particle distance, ρ/h . In fact, the bandwidth of the stiffness matrix increases with the ratio ρ/h (more particles lie inside the circle of radius ρ), see for instance Figure 5. Note that, for linear consistency, when ρ/h goes to 1, the linear finite element shape functions are recovered.*

Remark 13 (Continuity) *If the weight function ϕ is \mathcal{C}^k then the EFG/MLS shape functions, and the RKPM shape functions, are \mathcal{C}^k , see Liu et al. (1997a). Thus, if the window function is a cubic spline, as shown in Figures 6 and 7, the first and second derivatives of the shape functions are well defined throughout the domain, even with linear consistency.*

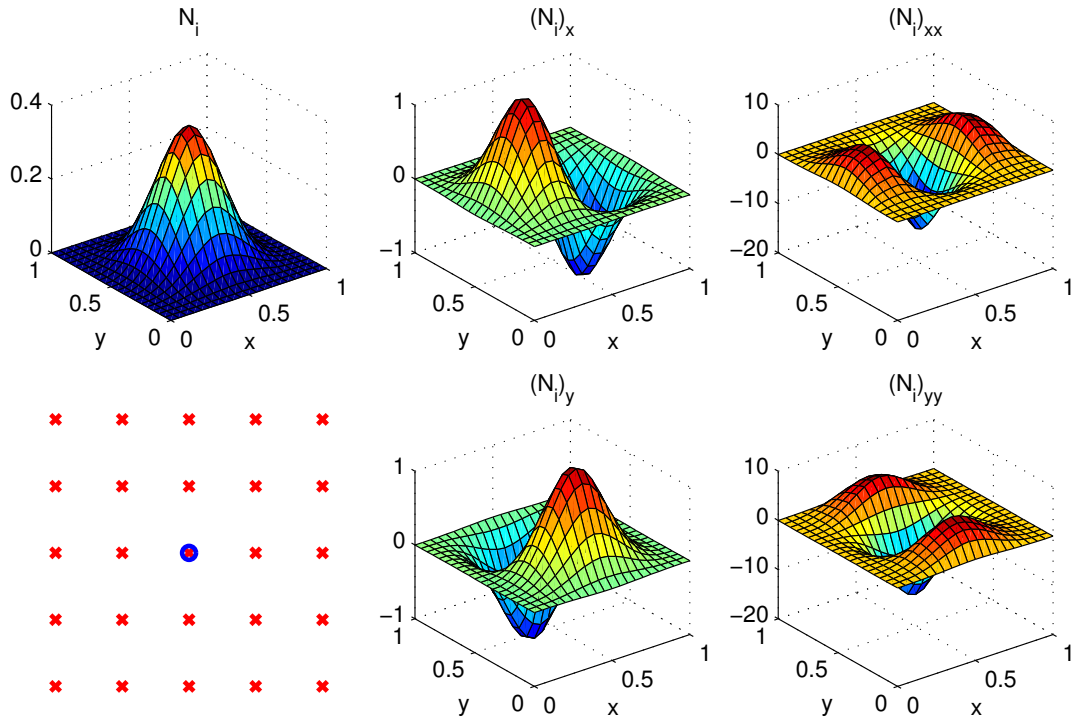


Figure 7. Distribution of particles, EFG approximation function and derivatives, with $\rho/h \simeq 2.2$ with circular supported cubic spline and linear consistency.

2.2.4. Reproducibility of the MLS approximation The MLS shape functions can be also obtained by imposing a priori the reproducibility properties of the approximation. Consider a set of particles \mathbf{x}_I and a complete polynomial base $\mathbf{P}(\mathbf{x})$. Let us assume an approximation of the form

$$u(\mathbf{x}) \simeq \sum_{I \in S_{\mathbf{x}}^p} N_I(\mathbf{x}) u(\mathbf{x}_I), \quad (27)$$

with approximation functions defined as

$$N_I(\mathbf{x}) = \omega(\mathbf{x}_I, \mathbf{x}) \mathbf{P}^T(\mathbf{x}_I) \boldsymbol{\alpha}(\mathbf{x}). \quad (28)$$

The unknown vector $\boldsymbol{\alpha}(\mathbf{x})$ in \mathbb{R}^{l+1} is determined imposing the reproducibility condition, which imposes that the approximation proposed in (27) is exact for all the polynomials in \mathbf{P} , namely

$$\mathbf{P}(\mathbf{x}) = \sum_{J \in S_{\mathbf{x}}^p} N_J(\mathbf{x}) \mathbf{P}(\mathbf{x}_J). \quad (29)$$

After substitution of (28) in (29), the linear system of equations that determines $\boldsymbol{\alpha}(\mathbf{x})$ is obtained

$$\mathbf{M}(\mathbf{x}) \boldsymbol{\alpha}(\mathbf{x}) = \mathbf{P}(\mathbf{x}). \quad (30)$$

That is,

$$\boldsymbol{\alpha}(\mathbf{x}) = \mathbf{M}^{-1}(\mathbf{x}) \mathbf{P}(\mathbf{x}), \quad (31)$$

where $\mathbf{M}(\mathbf{x})$ is the same matrix defined in (19). Finally, the approximation functions $N_I(\mathbf{x})$ are defined by substituting in (28) the vector $\boldsymbol{\alpha}$, see (31). Note that with this substitution the expression (18) for the MLS approximation functions is recovered, and consistency is ensured by construction.

Section 2.2.7 is devoted to some implementation details of the EFG method. In particular, it is shown that the derivatives of $N_I(\mathbf{x})$ can be computed without excessive overhead.

2.2.5. MLS centered and scaled approach For computational purposes, it is usual and preferable to center in \mathbf{x}_J and scale with ρ also the polynomials involved in the definition of the mesh-free approximation functions, see Liu *et al.* (1997a) or Huerta and Fernández-Méndez (2000). Thus, another expression for the EFG shape functions is employed:

$$N_I(\mathbf{x}) = \omega(\mathbf{x}_I, \mathbf{x}) \mathbf{P}^\top \left(\frac{\mathbf{x}_I - \mathbf{x}}{\rho} \right) \boldsymbol{\alpha}(\mathbf{x}), \quad (32)$$

which is similar to (28). Recall also that typical expressions for the window function are of the following type: $\phi(\mathbf{y}, \mathbf{x}) = \phi((\mathbf{y} - \mathbf{x})/\rho)$. The consistency condition becomes in this case:

$$\mathbf{P}(0) = \sum_{I \in S_{\mathbf{x}}^{\rho}} N_I(\mathbf{x}) \mathbf{P} \left(\frac{\mathbf{x}_I - \mathbf{x}}{\rho} \right), \quad (33)$$

which is equivalent to condition (29) when ρ is constant everywhere (see Remark 14 for non constant ρ). After substitution of (32) in (33) the linear system of equations that determines $\boldsymbol{\alpha}(\mathbf{x})$ is obtained:

$$\mathbf{M}(\mathbf{x}) \boldsymbol{\alpha}(\mathbf{x}) = \mathbf{P}(0), \quad (34)$$

where

$$\mathbf{M}(\mathbf{x}) = \sum_{J \in S_{\mathbf{x}}^{\rho}} \omega(\mathbf{x}_J, \mathbf{x}) \mathbf{P} \left(\frac{\mathbf{x}_J - \mathbf{x}}{\rho} \right) \mathbf{P}^\top \left(\frac{\mathbf{x}_J - \mathbf{x}}{\rho} \right). \quad (35)$$

Remark 14. *The consistency conditions (29) and (33) are equivalent if the dilation parameter ρ is constant. When the dilation parameter varies at each particle the same expression for $N_I(\mathbf{x})$ is used, namely equation (28), but the varying dilation parameter, ρ_I associated to particle \mathbf{x}_I , is imbedded in the definition of the weighting function; that is, equation (22) is modified as follows*

$$\omega(\mathbf{x}_I, \mathbf{x}) = \phi \left(\frac{\mathbf{x}_I - \mathbf{x}}{\rho_I} \right).$$

Note that a constant ρ is employed in the scaling of the polynomials \mathbf{P} . The constant value ρ is typically chosen as the mean value of all the ρ_J . The consistency condition in this case is also (33). It also imposes the reproducibility of the polynomials in \mathbf{P} .

This centered expression for the EFG shape functions can also be obtained with a discrete MLS development with the discrete centered scalar product

$$\langle f, g \rangle_{\mathbf{x}} = \sum_{J \in S_{\mathbf{x}}^{\rho}} \omega(\mathbf{x}_J, \mathbf{x}) f \left(\frac{\mathbf{x}_J - \mathbf{x}}{\rho} \right) g \left(\frac{\mathbf{x}_J - \mathbf{x}}{\rho} \right). \quad (36)$$

The MLS development in this case is as follows: fixed \mathbf{x} , for \mathbf{z} near \mathbf{x} , u is approximated as

$$u(\mathbf{z}) \simeq u^{\rho}(\mathbf{z}, \mathbf{x}) = \mathbf{P}^\top \left(\frac{\mathbf{z} - \mathbf{x}}{\rho} \right) \mathbf{c}(\mathbf{x}) \quad (37)$$

where \mathbf{c} is obtained, as usual, through a least-squares fitting with the discrete centered scalar product (36).

2.2.6. The diffuse derivative The centered MLS allows, with a proper definition of the polynomial basis \mathbf{P} , the reinterpretation of the coefficients in $\mathbf{c}(\mathbf{x})$ as approximations of u and its derivatives at the fixed point \mathbf{x} .

The approximation of the derivative of u in each spatial direction is the corresponding derivative of u^ρ . This requires to derive (21), that is

$$\frac{\partial u}{\partial \mathbf{x}} \simeq \frac{\partial u^\rho}{\partial \mathbf{x}} = \frac{\partial \mathbf{P}^\top}{\partial \mathbf{x}} \mathbf{c} + \mathbf{P}^\top \frac{\partial \mathbf{c}}{\partial \mathbf{x}}. \quad (38)$$

On one hand, the second term on the r.h.s. is not trivial. Derivatives of the coefficients \mathbf{c} require the resolution of a linear system of equations with the same matrix \mathbf{M} . As noted by Belytschko *et al.* (1996b) this is not an expensive task, see also Section 2.2.7. However, it requires the knowledge of the cloud of particles surrounding each point \mathbf{x} , and, thus, it depends on the point where derivatives are evaluated.

On the other hand, the first term is easily evaluated. The derivative of the polynomials in \mathbf{P} is trivial and can be evaluated *a priori*, without knowledge of the cloud of particles surrounding each point \mathbf{x} .

Villon (1991) and Nayroles *et al.* (1992) propose the concept of diffuse derivative, which consists in approximating the derivative only with the first term on the r.h.s. of (38), namely

$$\frac{\delta u^\rho}{\delta \mathbf{x}} = \frac{\partial u^\rho}{\partial \mathbf{z}} \Big|_{\mathbf{z}=\mathbf{x}} = \frac{\partial \mathbf{P}^\top}{\partial \mathbf{z}} \Big|_{\mathbf{z}=\mathbf{x}} \mathbf{c}(\mathbf{x}) = \frac{\partial \mathbf{P}^\top}{\partial \mathbf{x}} \mathbf{c}(\mathbf{x}).$$

From a computational cost point of view, this is an interesting alternative to (38). Moreover, the following proposition ensures convergence at optimal rate of the diffuse derivative.

Proposition 2. *If u^ρ is an approximation to u with an order of consistency m (i.e., \mathbf{P} includes a complete basis of the subspace of polynomials of degree m) and ρ/h is constant, then*

$$\left\| \frac{\partial^{|\mathbf{k}|} u}{\partial \mathbf{x}^{\mathbf{k}}} - \frac{\delta^{|\mathbf{k}|} u^\rho}{\delta \mathbf{x}^{\mathbf{k}}} \right\|_\infty \leq C(\mathbf{x}) \frac{\rho^{m+1-|\mathbf{k}|}}{(m+1)!} \quad \forall |\mathbf{k}| = 0, \dots, m. \quad (39)$$

where \mathbf{k} is a multi-index, $\mathbf{k} = (k_1, k_2, \dots, k_{n_{sd}})$ and $|\mathbf{k}| = k_1 + k_2 + \dots + k_{n_{sd}}$.

The proof can be found in Villon (1991) for 1D or Huerta *et al.* (2004a) for higher spatial dimensions. To clearly identify the coefficients of \mathbf{c} with the approximations of u and its derivatives the basis in \mathbf{P} should be written appropriately. That is, each component of \mathbf{P} is $P_\alpha(\boldsymbol{\xi}) = \boldsymbol{\xi}^\alpha / \alpha!$ for $|\alpha| = 0, \dots, m$, where a standard a multi-index notation is employed,

$$\mathbf{h}^\alpha := h_1^{\alpha_1} h_2^{\alpha_2} \dots h_{n_{sd}}^{\alpha_{n_{sd}}}; \quad \alpha! := \alpha_1! \alpha_2! \dots \alpha_{n_{sd}}!; \quad |\alpha| = \alpha_1 + \alpha_2 + \dots + \alpha_{n_{sd}}.$$

Finally, it is important to emphasize the requirements that \mathbf{M} is regular and bounded (see Huerta *et al.*, 2002; Fernández-Méndez and Huerta, 2002; Fernández-Méndez *et al.*, 2003).

Remark 15. *For example, in 1D with consistency of order two, i.e. $\mathbf{P}(\mathbf{x}) = \{1, \rho x, (\rho x)^2/2\}$, the expression (37) can be written as*

$$u(z) \simeq u^\rho(z, x) = c_0(x) + c_1(x)(z - x) + c_2(x)(z - x)^2/2. \quad (40)$$

Thus, deriving with respect to z and imposing $z = x$,

$$u(x) \simeq c_0(x), \quad u'(x) \simeq c_1(x) \quad \text{and} \quad u''(x) \simeq c_2(x).$$

In fact, this strategy is at the basis of the *diffuse element method*: the diffuse derivative is used in the weak form of the problem (see Nayroles *et al.*, 1992; Breiokopf *et al.*, 2001). Moreover, the *generalized finite difference* interpolation or *meshless finite difference method*, see Orkisz (1998), coincides also with this MLS development. The only difference between the generalized finite difference interpolation and the EFG centered interpolation is the definition of the set of neighboring particles $S_{\mathbf{x}}^p$.

2.2.7. Direct evaluation of the derivatives Another alternative to compute the derivatives is to fully derive the expression for the shape function (28), see (38), taking into account the dependencies given by equations (30) and (19). The details can found in the references by Belytschko *et al.* (1996a,1996b).

For clarity the 1D case is developed, $x \in \mathbb{R}$, for higher dimensions the process is repeated for each component of \mathbf{x} . The derivative of the shape function (28) can be written as

$$\frac{dN_I}{dx}(x) = \omega(x_I, x) \mathbf{P}^\top(x_I) \frac{d\boldsymbol{\alpha}}{dx}(x) + \frac{d\omega(x_I, x)}{dx} \mathbf{P}^\top(x_I) \boldsymbol{\alpha}(x). \quad (41)$$

The derivative of the weighting function is easily obtained because $\omega(x_I, x)$ has usually known analytical expressions, see (22) and Section 2.1.2. The a priori not trivial part is the evaluation of $d\boldsymbol{\alpha}/dx$, but an expression for this vector can be obtained by implicit derivation of (30),

$$\mathbf{M}_x(x) \boldsymbol{\alpha}(x) + \mathbf{M}(x) \frac{d\boldsymbol{\alpha}}{dx}(x) = \frac{d\mathbf{P}}{dx}(x),$$

where matrix \mathbf{M}_x is the derivative of matrix \mathbf{M} ,

$$\mathbf{M}_x(x) = \sum_J \frac{d\omega(x_J, x)}{dx} \mathbf{P}(x_J) \mathbf{P}^\top(x_J),$$

which is trivial to compute. Thus, $d\boldsymbol{\alpha}/dx$ is the solution of the linear system of equations

$$\mathbf{M}(x) \frac{d\boldsymbol{\alpha}}{dx}(x) = \frac{d\mathbf{P}}{dx}(x) - \mathbf{M}_x(x) \boldsymbol{\alpha}(x),$$

which represents another linear system of equations with the same matrix that in (30) (the factorization of \mathbf{M} can be reused) and a new independent term. Moreover, the product $\mathbf{M}_x(x)\boldsymbol{\alpha}(x)$ can be computed in an efficient way as

$$\mathbf{M}_x(x)\boldsymbol{\alpha}(x) = \sum_J \frac{d\omega(x_J, x)}{dx} \mathbf{P}(x_J) [\mathbf{P}^\top(x_J)\boldsymbol{\alpha}(x)],$$

involving only vector operations.

In summary, the evaluation of the derivatives of the shape functions, see (41), requires little extra computer cost and, moreover, higher order derivatives can also be computed repeating the same process, it only depends on the regularity of $\omega(x_I, x)$. Obviously, the same development can be done for the centered and scaled approach defined in Section 2.2.5.

2.2.8. Partition of the unity methods The set of MLS approximation functions can be viewed as a partition of unity: the approximation verifies, at least, the 0-order consistency condition (reproducibility of the constant polynomial $p(\mathbf{x}) = 1$)

$$\sum_I N_I \cdot 1 = 1.$$

This viewpoint leads to new approximations for mesh-free methods. Based on the *partition of the unity finite element method* (PUFEM) proposed by Babuška and Melenk (1995), Duarte and Oden (1996a) use the concept of partition of unity to construct approximations with consistency of order $k \geq 1$. They called their method *h-p clouds*. The approximation is

$$u(\mathbf{x}) \simeq u^\rho(\mathbf{x}) = \sum_I N_I(\mathbf{x})u_I + \sum_I \sum_{i=1}^{n_I} b_{Ii} [N_I(\mathbf{x}) q_{Ii}(\mathbf{x})],$$

where $N_I(\mathbf{x})$ are the MLS approximation functions, q_{Ii} are n_I polynomials of degree greater than k associated to each particle \mathbf{x}_I , and u_I, b_{Ii} are coefficients to determine. Note that the polynomials $q_{Ii}(\mathbf{x})$ increase the order of the approximation space. These polynomials can be different from particle to particle, thus facilitating the hp-adaptivity.

Remark 16. *As commented in Belytschko et al. (1996a), the concept of an extrinsic basis, $q_{Ii}(\mathbf{x})$, is essential for obtaining p-adaptivity. In MLS approximations, the intrinsic basis \mathbf{P} cannot vary from particle to particle without introducing a discontinuity.*

3. DISCRETIZATION OF PARTIAL DIFFERENTIAL EQUATIONS

All the approximation functions described in the previous section can be used in the solution of a PDE boundary value problem. Usually SPH methods are combined with collocation or point integration technique, while the approximations based on MLS are usually combined with a Galerkin discretization.

A large number of published methods with minor differences exist. Probably, the best known, among those using MLS approximation, are: the *meshless (generalized) finite difference method* (MFDG) developed by Liszka and Orkisz (1980), the *diffuse element method* (DEM) by Nayroles et al. (1992), the *element-free Galerkin* (EFG) method by Belytschko et al. (1994), the *reproducing kernel particle method* (RKPM) by Liu et al. (1995a), the *meshless local Petrov-Galerkin* (MLPG) by Zhu and Atluri (1998), the *corrected smooth particle hydrodynamics* (CSPH) by Bonet and Lok (1999) and the *finite point method* (FPM) by Oñate and Idelsohn (1998). Table I classifies these methods depending on the evaluation of the derivatives (see Sections 2.2.6 and 2.2.7) and how the PDE is solved (Galerkin, Petrov-Galerkin, point collocation).

Partition of unity methods can be implemented with Galerkin, Petrov-Galerkin, etc. For instance, the *h-p clouds* by Duarte and Oden (1996a) use a Galerkin weak form with accurate integration, while the *finite spheres* by De and Bathe (2000) uses Shepard functions (with circular/spherical support) enriched with polynomials and a Galerkin weak form with specific quadratures for spherical domains (and particular/adapted quadratures near the boundary); almost identical to h-p clouds Duarte and Oden (1996a).

In order to discuss some of these methods in more detail, the model boundary value problem

$$\Delta u - u = -f \quad \text{in } \Omega \quad (42a)$$

$$u = u_D \quad \text{on } \Gamma_D \quad (42b)$$

$$\frac{\partial u}{\partial \mathbf{n}} = g_N \quad \text{on } \Gamma_N \quad (42c)$$

Table I. Classification of MLS based mesh-free methods for PDE's

		Evaluation of derivatives	
		Consistent	Diffuse
Galerkin	Gauss quadrature	EFG RKPM	MFDM DEM
	particle quadrature	CSHP*	
Petrov-Galerkin		MLPG	
Point Collocation			FPM

* Consistent and global evaluation of derivatives.

is considered, where Δ is the Laplace operator in 2D, $\Delta \cdot = \partial^2 \cdot / \partial x^2 + \partial^2 \cdot / \partial y^2$, \mathbf{n} is the unitary outward normal vector on $\partial\Omega$, $\partial/\partial\mathbf{n}$ is the normal derivative, $\partial \cdot / \partial \mathbf{n} = n_1 \partial \cdot / \partial x + n_2 \partial \cdot / \partial y$, $\bar{\Gamma}_D \cup \bar{\Gamma}_N = \partial\Omega$, and f , u_D and g_N are known.

Remark 17. *A major issue in the implementation of mesh-free methods is the identification (localization) of the neighboring particles. That is, given a point \mathbf{x} in the domain, identify which particles have a non-zero shape function at this point, i.e. determine the \mathbf{x}_I such that $\phi((\mathbf{x}_I - \mathbf{x})/\rho) \neq 0$ to define S_x^ρ .*

There are several options. The usual ones consist in determining the closest particles to the point of interest (see Randles and Libersky, 2000) or to use a non conforming regular mesh of squares or cubes (cells) parallel to the cartesian axes. For every cell, the indices of the particles inside the cell are stored. The regular structure of the cell mesh allows to find, given a point \mathbf{x} , the cell where \mathbf{x} is located and thus, determine the neighboring particles just looking in the neighboring cells. Fast algorithms for finding neighboring particles can be found in the book by Schweitzer (2003).

3.1. Collocation methods

Consider an approximation, based on a set of particles $\{\mathbf{x}_I\}$, of the form

$$u(\mathbf{x}) \simeq u^\rho(\mathbf{x}) = \sum_I u_I N_I(\mathbf{x}).$$

The shape functions $N_I(\mathbf{x})$ can be SPH shape functions (Section 2.1.1), or MLS shape functions (Section 2.2), and u_I are coefficients to be determined.

In collocation methods, see Oñate and Idelsohn (1998) or Aluru (2000), the PDE (42a) is imposed at each particle in the interior of the domain Ω , the boundary conditions (42b) and (42c) are imposed at each particle of the corresponding boundary. In the case of the model

problem, this leads to the linear system of equations for the coefficients u_I :

$$\begin{cases} \sum_I u_I [\Delta N_I(\mathbf{x}_J) - N_I(\mathbf{x}_J)] = -f(\mathbf{x}_J) & \forall \mathbf{x}_J \in \Omega, \\ \sum_I u_I N_I(\mathbf{x}_J) = u_D(\mathbf{x}_J) & \forall \mathbf{x}_J \in \Gamma_D, \\ \sum_I u_I \frac{\partial N_I}{\partial \mathbf{n}}(\mathbf{x}_J) = g_N(\mathbf{x}_J) & \forall \mathbf{x}_J \in \Gamma_N. \end{cases}$$

Note that, the shape functions must be \mathcal{C}^2 , and thus, a \mathcal{C}^2 window function must be used. In this case the solution at particle \mathbf{x}_J is approximated by

$$u(\mathbf{x}_J) \simeq u^\rho(\mathbf{x}_J) = \sum_I u_I N_I(\mathbf{x}_J),$$

which in general differs from the coefficient u_J (see Remark 1).

In the context of the renormalized meshless derivative (see Vila, 1999) the coefficient u_J is considered as the approximation at the particle \mathbf{x}_J and only the derivative of the solution is approximated through the RMD, see (9). Thus, the linear system to be solved becomes

$$\begin{cases} \sum_I u_I \Delta N_I(\mathbf{x}_J) - u_J = -f(\mathbf{x}_J) & \forall \mathbf{x}_J \in \Omega, \\ u_J = u_D(\mathbf{x}_J) & \forall \mathbf{x}_J \in \Gamma_D, \\ \sum_I u_I \frac{\partial N_I}{\partial \mathbf{n}}(\mathbf{x}_J) = g_N(\mathbf{x}_J) & \forall \mathbf{x}_J \in \Gamma_N. \end{cases}$$

Both possibilities are slightly different from the SPH method by Monaghan (1988) or from SPH methods based on particle integration techniques Bonet and Kulasegaram (2000).

3.2. Methods based on a Galerkin weak form

The mesh-free shape functions can also be used in the discretization of the weak integral form of the boundary value problem. For the model problem (42), the Bubnov-Galerkin weak form (also used in the finite element method) is

$$\int_{\Omega} \nabla v \nabla u \, d\Omega + \int_{\Omega} v u \, d\Omega = \int_{\Omega} v f \, dv + \int_{\Gamma_N} v g_N \, d\Gamma \quad \forall v,$$

where v vanishes at Γ_D and $u = u_D$ at Γ_D . However, this weak form can not be directly discretized with a standard mesh-free approximation. The shape functions do not verify the Kronecker delta property (see Remark 1) and thus, it is difficult to select v such that $v = 0$ at Γ_D and to impose that $u^\rho = u_D$ at Γ_D . Specific techniques are needed in order to impose Dirichlet boundary conditions. Section 3.3 describes to the treatment of essential boundary conditions in mesh-free methods.

An important issue in the implementation of a mesh-free method with a weak form is the evaluation of integrals in the weak form (the concept of finite element, with a numerical quadrature in each element can not be adopted directly).

Several possibilities can be considered to evaluate integrals in the weak form: (1) the particles can be the quadrature points (*particle integration*), (2) a regular cell structure (for instance,

the same used for the localization of particles) can be used with numerical quadrature in each cell (*cell integration*) or (3) a, not necessary regular, *background mesh* can be used to compute integrals. The first possibility (particle integration) is the fastest, but as in collocation methods it can result in rank deficiency. Bonet and Kulasegaram (2000) propose a global correction to obtain accurate and stable results with particle integration. The other two possibilities present the disadvantage that, since shape functions and their derivatives, are not polynomials, the number of integration points leads to high computational costs. Nevertheless, the cell structure or the coarse background mesh, which do not need to be conforming, are easily generated and these techniques ensure an accurate approximation of the integrals.

3.3. Essential boundary conditions

Many specific techniques have been developed in the recent years in order to impose essential boundary conditions in mesh-free methods. Some possibilities are: (1) Lagrange multipliers (Belytschko *et al.*, 1994), (2) modified variational principles (Belytschko *et al.*, 1994), (3) penalty methods (Zhu and Atluri, 1998; Bonet and Kulasegaram, 2000), (4) perturbed Lagrangian (Chu and Moran, 1995), (5) coupling to finite elements (Belytschko *et al.*, 1995; Huerta and Fernández-Méndez, 2000; Wagner and Liu, 2001), or (6) modified shape functions (Gosz and Liu, 1996; Günter and Liu, 1998; Wagner and Liu, 2000) among others.

The first attempts to define shape functions with the “delta property” along the boundary (see Gosz and Liu, 1996), namely $N_I(\mathbf{x}_J) = \delta_{IJ}$ for all \mathbf{x}_J in Γ_D , have serious difficulties for complex domains and for the integration of the weak forms.

In the recent years, mixed interpolations that combine finite elements with mesh-free methods have been developed. Mixed interpolations can be quite effective for imposing essential boundary conditions. The idea is to use one or two layers of finite elements next to the Dirichlet boundary and use a mesh-free approximation in the rest of the domain. Thus, the essential boundary conditions can be imposed as in standard finite elements. In Belytschko *et al.* (1995) a mixed interpolation is defined in the transition area (from the finite elements region to the particles region). This mixed interpolation requires the substitution of finite element nodes by particles and the definition of ramp functions. Thus, the transition is of the size of one element and the interpolation is linear. Following this idea, Huerta and Fernández-Méndez (2000) propose a more general mixed interpolation, with any order of interpolation, with no need for ramp functions and no substitution of nodes by particles. This is done preserving consistency and continuity of the solution. Figure 8 shows an example of this mixed interpolation in 1D: two finite element nodes are considered at the boundary of the domain, with their corresponding shape functions in blue, and the mesh-free shape functions are modified in order to preserve consistency, in black. The details of this method are presented in Section 6.

3.3.1. Methods based on a modification of the weak form For the sake of clarity, the following model problem is considered

$$\begin{cases} -\Delta u = f & \text{in } \Omega \\ u = u_D & \text{on } \Gamma_D \\ \nabla u \cdot \mathbf{n} = g_N & \text{on } \Gamma_N \end{cases} \quad (43)$$

where $\bar{\Gamma}_D \cup \bar{\Gamma}_N = \partial\Omega$, $\bar{\Gamma}_D \cap \bar{\Gamma}_N = \emptyset$ and \mathbf{n} is the outward unit normal on $\partial\Omega$. The generalization of the following developments to other PDEs is straightforward.

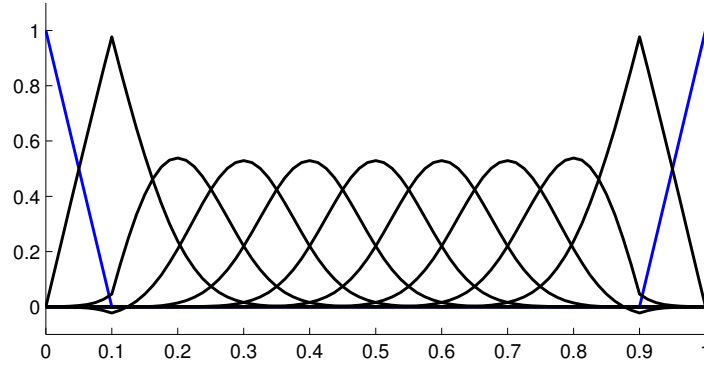


Figure 8. Mixed interpolation with linear finite element nodes near the boundary and particles in the interior of the domain, with $\rho/h = 3.2$, cubic spline and linear consistency in all the domain.

The weak problem form of (43) is “find $u \in \mathcal{H}^1(\Omega)$ such that $u = u_D$ on Γ_D and

$$\int_{\Omega} \nabla v \cdot \nabla u \, d\Omega - \int_{\Gamma_D} v \nabla u \cdot \mathbf{n} \, d\Gamma = \int_{\Omega} v f \, d\Omega + \int_{\Gamma_N} v g_N \, d\Gamma, \quad (44)$$

for all $v \in \mathcal{H}^1(\Omega)$ ”. In the finite element method, the interpolation of u can easily be forced to verify the essential boundary condition, and the test functions v can be chosen such that $v = 0$ on Γ_D (see Remark 18), leading to the following weak form: “find $u \in \mathcal{H}^1(\Omega)$ such that $u = u_D$ on Γ_D and

$$\int_{\Omega} \nabla v \cdot \nabla u \, d\Omega = \int_{\Omega} v f \, d\Omega + \int_{\Gamma_N} v g_N \, d\Gamma, \quad (45)$$

for all $v \in \mathcal{H}_0^1(\Omega)$ ”, where $\mathcal{H}_0^1(\Omega) = \{v \in \mathcal{H}^1(\Omega) \mid v = 0 \text{ on } \Gamma_D\}$.

Remark 18. In the finite element method, or in the context of the continuous blending method discussed in Section 6, the approximation can be written as

$$u(x) \simeq \sum_{j \notin \mathcal{B}} u_j N_j(x) + \psi(x) \quad (46)$$

where $N_j(x)$ denote the shape functions, $\psi(x) = \sum_{j \in \mathcal{B}} u_D(x_j) N_j(x)$, and \mathcal{B} is the set of indexes of all nodes on the essential boundary. Note that, due to the Kronecker delta property of the shape functions for $i \in \mathcal{B}$, and the fact that $N_i \in \mathcal{H}_0^1(\Omega)$ for $i \notin \mathcal{B}$, the approximation defined by (46) verifies $u = u_D$ at the nodes on the essential boundary. Therefore, approximation (46) and $v = N_i$, for $i \notin \mathcal{B}$, can be considered for the discretization of the weak form (45). Under these circumstances, the system of equations becomes

$$\mathbf{K}\mathbf{u} = \mathbf{f}, \quad (47)$$

where

$$\begin{aligned} K_{ij} &= \int_{\Omega} \nabla N_i \cdot \nabla N_j \, d\Omega, \\ f_i &= \int_{\Omega} N_i f \, d\Omega + \int_{\Omega} N_i \psi \, d\Omega + \int_{\Gamma_N} N_i g_N \, d\Gamma, \end{aligned} \quad (48)$$

and \mathbf{u} is the vector of coefficients u_i .

However, for standard mesh-free approximation, the shape functions do not verify the Kronecker delta property and $N_i \notin \mathcal{H}_0^1(\Omega)$ for $i \notin \mathcal{B}$. Therefore, imposing $u = u_D$ and $v = 0$ on Γ_D is not as straightforward as in finite elements or as in the blending method (Belytschko *et al.*, 1995), and the weak form defined by (45) cannot be used. The most popular methods that modify the weak form to overcome this problem are: the Lagrange multiplier method, the penalty method and Nitsche's method.

3.3.2. Lagrange multiplier method The solution of problem (43) can also be obtained as the solution of a minimization problem with constraints: “ u minimizes the energy functional

$$\Pi(v) = \frac{1}{2} \int_{\Omega} \nabla v \cdot \nabla v \, d\Omega - \int_{\Omega} v f \, d\Omega - \int_{\Gamma_N} v g_N \, d\Gamma, \quad (49)$$

and verifies the essential boundary conditions.” That is,

$$u = \arg \min_{\substack{v \in \mathcal{H}^1(\Omega) \\ v = u_D \text{ on } \Gamma_D}} \Pi(v). \quad (50)$$

With the use of a Lagrange multiplier, $\lambda(x)$, this minimization problem can also be written as

$$(u, \lambda) = \arg \min_{v \in \mathcal{H}^1(\Omega)} \max_{\gamma \in \mathcal{H}^{-1/2}(\Gamma_D)} \Pi(v) + \int_{\Gamma_D} \gamma (v - u_D) \, d\Gamma.$$

This min-max problem leads to the following weak form with Lagrange multiplier, “find $u \in \mathcal{H}^1(\Omega)$ and $\lambda \in \mathcal{H}^{-1/2}(\Gamma_D)$ such that

$$\int_{\Omega} \nabla v \cdot \nabla u \, d\Omega + \int_{\Gamma_D} v \lambda \, d\Gamma = \int_{\Omega} v f \, d\Omega + \int_{\Gamma_N} v g_N \, d\Gamma, \quad \forall v \in \mathcal{H}^1(\Omega) \quad (51a)$$

$$\int_{\Gamma_D} \gamma (u - u_D) \, d\Gamma = 0, \quad \forall \gamma \in \mathcal{H}^{-\frac{1}{2}}(\Gamma_D).” \quad (51b)$$

Remark 19. Equation (51b) imposes the essential boundary condition, $u = u_D$ on Γ_D , in weak form.

Remark 20. The physical interpretation of the Lagrange multiplier can be seen by simple comparison of equations (51a) and (44): the Lagrange multiplier corresponds to the flux (traction in a mechanical problem) along the essential boundary, $\lambda = -\nabla u \cdot \mathbf{n}$.

Considering now the approximation $u(x) \simeq \sum_i N_i(x) u_i$, with mesh-free shape functions N_i , and an interpolation for λ with a set of boundary functions $\{N_i^L(x)\}_{i=1}^{\ell}$,

$$\lambda(x) \simeq \sum_{i=1}^{\ell} \lambda_i N_i^L(x) \quad \text{for } x \in \Gamma_D, \quad (52)$$

the discretization of (51) leads to the system of equations

$$\begin{pmatrix} \mathbf{K} & \mathbf{A}^T \\ \mathbf{A} & \mathbf{0} \end{pmatrix} \begin{pmatrix} \mathbf{u} \\ \boldsymbol{\lambda} \end{pmatrix} = \begin{pmatrix} \mathbf{f} \\ \mathbf{b} \end{pmatrix}, \quad (53)$$

where \mathbf{K} and \mathbf{f} are already defined in (48) (use $\psi = 0$), $\boldsymbol{\lambda}$ is the vector of coefficients λ_i , and

$$A_{ij} = \int_{\Gamma_D} N_i^L N_j \, d\Gamma, \quad b_i = \int_{\Gamma_D} N_i^L u_D \, d\Gamma.$$

There are several possibilities for the choice of the interpolation space for the Lagrange multiplier λ . Some of them are (1) a finite element interpolation on the essential boundary, (2) a mesh-free approximation on the essential boundary or (3) the same shape functions used in the interpolation of u restricted along Γ_D , i.e. $N_i^L = N_i$ for i such that $N_i|_{\Gamma_D} \neq 0$. However, the most popular choice is the point collocation method. This method corresponds to $N_i^L(x) = \delta(x - x_i^L)$, where $\{x_i^L\}_{i=1}^{\ell}$ is a set of points along Γ_D and δ is the Dirac delta function. In that case, by substitution of $\gamma(x) = \delta(x - x_i^L)$, equation (51b) corresponds to

$$u(x_i^L) = u_D(x_i^L), \quad \text{for } i = 1 \dots \ell.$$

That is, $A_{ij} = N_j(x_i^L)$, $b_i = u_D(x_i^L)$, and each equation of $\mathbf{A}\mathbf{u} = \mathbf{b}$ in (53) corresponds to the enforcement of the prescribed value at one collocation point, namely x_i^L .

Remark 21. *The system of equations (53) can also be derived from the minimization in $\mathbb{R}^{n_{\text{dof}}}$ of the discrete version of the energy functional (49) subject to the constraints corresponding to the essential boundary conditions, $\mathbf{A}\mathbf{u} = \mathbf{b}$. In fact, there is no need to know the weak form with Lagrange multiplier, it is sufficient to define the discrete energy functional and the restrictions due to the boundary conditions in order to determine the system of equations.*

Therefore, the Lagrange multiplier method is, in principle, general and easily applicable to all kind of problems. However, the main disadvantages of the Lagrange multiplier method are:

1. The dimension of the resulting system of equations is increased.
2. Even for \mathbf{K} symmetric and semi-positive definite, the global matrix in (53) is symmetric but it is no longer positive definite. Therefore, standard linear solvers for symmetric and positive definite matrices can not be used.
3. More crucial is the fact that the system (53) and the weak problem (51) induce a saddle point problem which precludes an arbitrary choice of the interpolation space for u and λ . The resolution of the multiplier λ field must be fine enough in order to obtain an acceptable solution, but the system of equations will be singular if the resolution of Lagrange multipliers λ field is too fine. In fact, the interpolation spaces for the Lagrange multiplier λ and for the principal unknown u must verify an inf-sup condition, known as the Babuska-Brezzi stability condition, in order to ensure the convergence of the approximation (see Babuska, 1973a or Brezzi, 1974 for details).

The first two disadvantages can be neglected in view of the versatility and simplicity of the method. However, while in the finite element method it is trivial to choose the approximation for the Lagrange multiplier in order to verify the Babuska-Brezzi stability condition and to impose accurate essential boundary conditions, this choice is not trivial for mesh-free methods. In fact, in mesh-free methods the choice of an appropriate interpolation for the Lagrange multiplier can be a serious problem in particular situations.

These properties are observed in the resolution of the 2D linear elasticity problem represented in Figure 9. Where the solution obtained with a regular mesh of 30×30 biquadratic finite elements is also shown. The distance between particles is $h = 1/6$ and a finer mesh is used for the representation of the solution.

Figure 10 shows the solution obtained for the Lagrange multiplier method. The prescribed displacement is imposed at some collocation points at the essential boundary (marked with black squares). Three possible distributions for the collocation points are considered. In the first one the collocation points correspond to the particles located at the essential boundary.

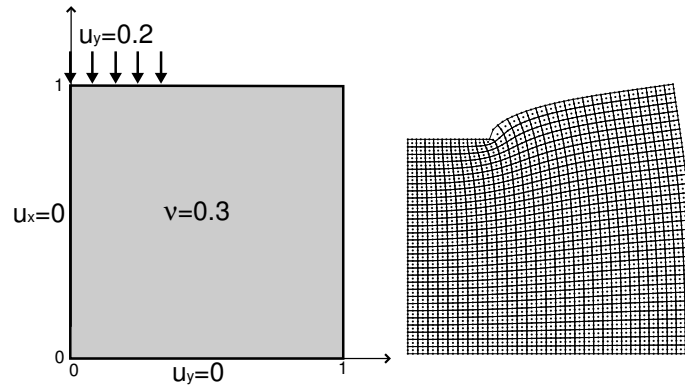


Figure 9. Problem statement and solution with 30×30 biquadratic finite elements (61×61 nodes)

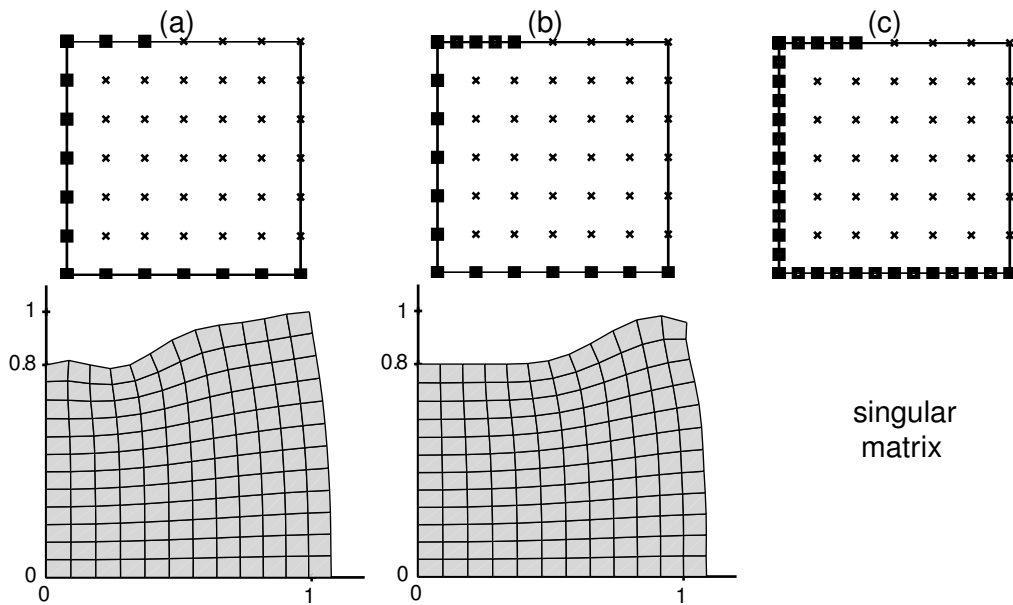


Figure 10. Solution with Lagrange multipliers for three possible distributions of collocation points (black squares) and 7×7 particles

The prescribed displacement is exactly imposed at the collocation points, but not along the rest of the essential boundary. Note that the displacement field is not accurate because of the smoothness of the mesh-free approximation. But if the number of collocation points is too large the inf-sup condition is no longer verified and the stiffness system matrix is singular. This is the case of discretization (c) which corresponds to double the density of collocation points along the essential boundary. In this example, the choice of a proper interpolation for the Lagrange multiplier is not trivial. Option (b) represents a distribution of collocation points that imposes the prescribed displacements in a correct manner and, at the same time, leads to

a regular matrix. Similar results are obtained if the Lagrange multiplier is interpolated with boundary linear finite elements (see Fernández-Méndez and Huerta, 2004).

Therefore, although imposing boundary constraints is straightforward with the Lagrange multiplier method, the applicability of this method in particular cases is impaired due to the difficulty in the selection of a proper interpolation space for the Lagrange multiplier. It is important to note that the choice of the interpolation space can be even more complicated for an irregular distribution of particles.

3.3.3. Penalty method The minimization problem with constraints defined by (50) can also be solved with the use of a penalty parameter. That is,

$$u = \arg \min_{v \in \mathcal{H}^1(\Omega)} \Pi(v) + \frac{1}{2} \beta \int_{\Gamma_D} (v - u_D)^2 \, d\Gamma. \quad (54)$$

The penalty parameter β is a positive scalar constant that must be large enough to accurately impose the essential boundary condition. The minimization problem (54) leads to the following weak form: “find $u \in \mathcal{H}^1(\Omega)$ such that

$$\int_{\Omega} \nabla v \cdot \nabla u \, d\Omega + \beta \int_{\Gamma_D} v u \, d\Gamma = \int_{\Omega} v f \, d\Omega + \int_{\Gamma_N} v g_N \, d\Gamma + \beta \int_{\Gamma_D} v u_D \, d\Gamma, \quad (55)$$

for all $v \in \mathcal{H}^1(\Omega)$ ”. The discretization of this weak form leads to the system of equations

$$(\mathbf{K} + \beta \mathbf{M}^p) \mathbf{u} = \mathbf{f} + \beta \mathbf{f}^p, \quad (56)$$

where \mathbf{K} and \mathbf{f} are defined in (48) (use $\psi = 0$) and

$$M_{ij}^p = \int_{\Gamma_D} N_i N_j \, d\Gamma, \quad f_i^p = \int_{\Gamma_D} N_i u_D \, d\Gamma.$$

Remark 22. *The penalty method can also be obtained from the minimization of the discrete version of the energy functional in $\mathbb{R}^{n_{\text{dof}}}$, subjected to the constraints corresponding to the essential boundary condition, $\mathbf{A} \mathbf{u} = \mathbf{b}$.*

Like the Lagrange multiplier method, the penalty method is easily applicable to a wide range of problems. The penalty method presents two clear advantages: (i) the dimension of the system is not increased and (ii) the matrix in the resulting system, see equation (56), is symmetric and positive definite, provided that \mathbf{K} is symmetric and β is large enough.

However, the penalty method also has two important drawbacks: the Dirichlet boundary condition is weakly imposed (the parameter β controls how well the essential boundary condition is met) and the matrix in (56) is often poorly conditioned (the condition number increases with β)

A general theorem on the convergence of the penalty method and the choice of the penalty parameter β can be found in Babuska (1973b) and Babuska *et al.* (2002). For an interpolation with consistency of order p and discretization measure h (i.e. the characteristic element size in finite elements or the characteristic distance between particles in a mesh-free method) the best error estimate obtained by Babuska (1973b) gives a rate of convergence of order $h^{\frac{2p+1}{3}}$ in the energy norm, provided that the penalty β is taken to be of order $h^{-\frac{2p+1}{3}}$. In the linear case, it corresponds to the optimal rate of convergence in the energy norm. For order $p \geq 2$, the lack

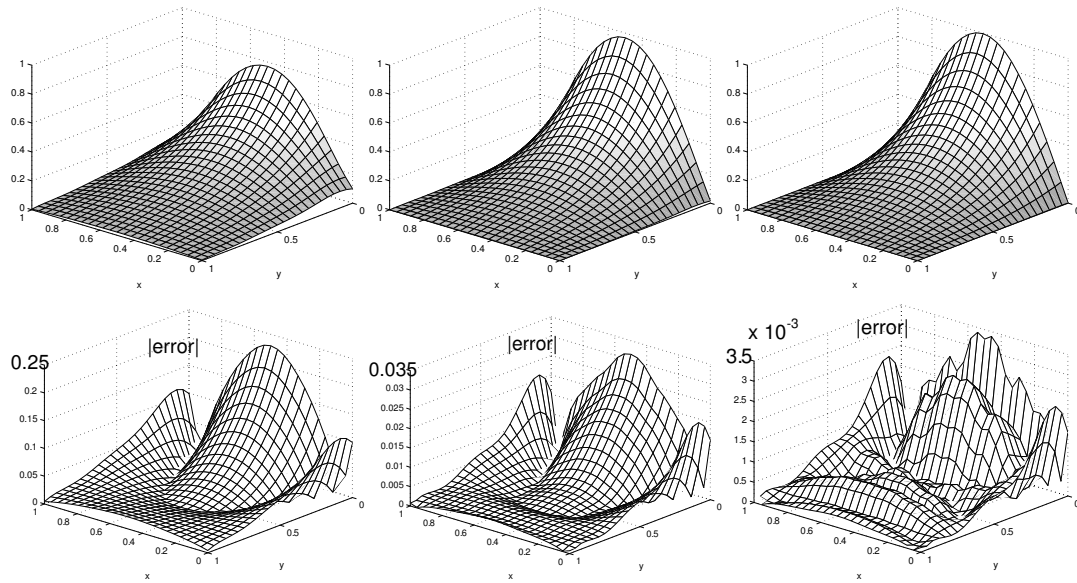


Figure 11. Penalty method solution (top) and error (bottom) for $\beta = 10$ (left), $\beta = 100$ (center) and $\beta = 10^3$ (right)

of optimality in the rate of convergence is a direct consequence of the lack of consistency of the weak formulation (see Arnold *et al.*, 2001/02 and Remark 23).

These properties can be observed in the following Laplace 2D problem

$$\begin{cases} \Delta u = 0 & (x, y) \in]0, 1[\times]0, 1[\\ u(x, 0) = \sin(\pi x) \\ u(x, 1) = u(0, y) = u(1, y) = 0 \end{cases}$$

with analytical solution (see Wagner and Liu, 2000),

$$u(x, y) = [\cosh(\pi y) - \coth(\pi y) \sinh(\pi y)] \sin(\pi x).$$

A distribution of 7×7 particles is considered, i.e. the distance between particles is $h = 1/6$.

Figure 11 shows the solution for increasing values of the penalty parameter β . The penalty parameter must be large enough, $\beta \geq 10^3$, in order to impose the boundary condition in an accurate manner. Figure 12 shows convergence curves for different choices of the penalty parameter. The penalty method converges with a rate close to 2 in the \mathcal{L}^2 norm if the penalty parameter β is proportional to h^{-2} . If the penalty parameter is constant, or proportional to h^{-1} , the boundary error dominates and the optimal convergence rate is lost as h goes to zero.

Figure 12 also shows the matrix condition number for increasing values of the penalty parameter, for a distribution of 11×11 and 21×21 particles. The condition number grows linearly with the penalty parameter. Note that, for instance, for a discretization with 21×21 a reasonable value for the penalty parameter is $\beta = 10^6$ which corresponds to a condition number near 10^{12} . Obviously, the situation gets worse for denser discretizations, which need larger penalty parameters. The ill-conditioning of the matrix reduces the applicability of the penalty method.

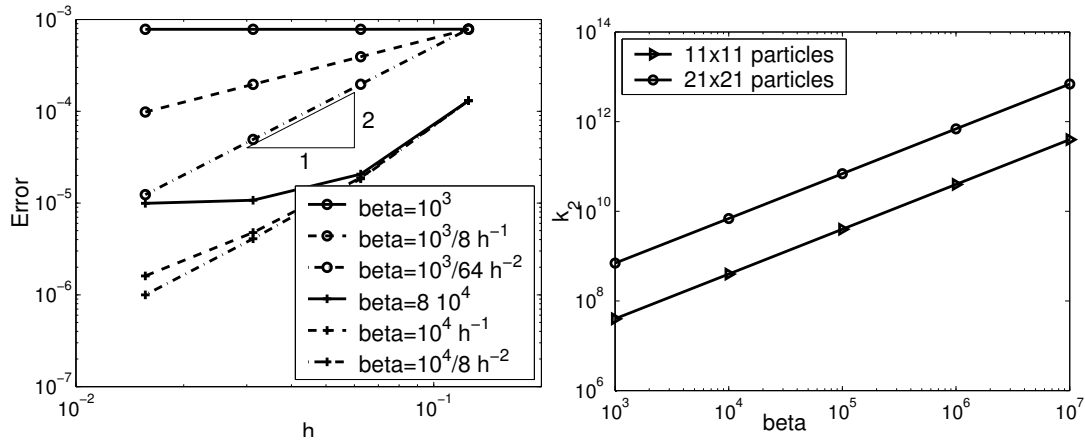


Figure 12. Evolution of the $\mathcal{L}^2(\Omega)$ error norm for the penalty method and matrix condition number

3.3.4. *Nitsche's method* Nitsche's weak form for problem (43) is

$$\begin{aligned} & \int_{\Omega} \nabla v \cdot \nabla u \, d\Omega - \int_{\Gamma_D} v \nabla u \cdot \mathbf{n} \, d\Gamma - \int_{\Gamma_D} \nabla v \cdot \mathbf{n} u \, d\Gamma + \beta \int_{\Gamma_D} v u \, d\Gamma \\ & = \int_{\Omega} v f \, d\Omega + \int_{\Gamma_N} v g_N \, d\Gamma - \int_{\Gamma_D} \nabla v \cdot \mathbf{n} u_D \, d\Gamma + \beta \int_{\Gamma_D} v u_D \, d\Gamma, \end{aligned} \quad (57)$$

where β is a positive constant scalar parameter (see Arnold *et al.*, 2001/02; Nitsche, 1970).

Comparing with the weak form defined by (44), the new terms in the l.h.s. of (57) are $\int_{\Gamma_D} u \nabla v \cdot \mathbf{n} \, d\Gamma$, which recovers the symmetry of the bilinear form, and $\beta \int_{\Gamma_D} v u \, d\Gamma$, that ensures the coercivity of the bilinear form (i.e. the matrix corresponding to its discretization is positive definite) provided that β is large enough. The new terms in the r.h.s. are added to ensure consistency of the weak form.

The discretization of the Nitsche's weak form leads to a system of equations with the same size as \mathbf{K} and whose matrix is symmetric and positive definite, provided that \mathbf{K} is symmetric and β is large enough. Although, as in the penalty method, the condition number of this matrix increases with parameter β , in practice not very large values are needed in order to ensure convergence and a proper implementation of the boundary condition.

Remark 23. *Nitsche's method can be interpreted as a consistent improvement of the penalty method. The penalty weak form (55) is not consistent, in the sense that the solution of (43) does not verify the penalty weak form for trial test functions that do not vanish at Γ_D (see Arnold *et al.*, 2001/02). Nitsche's weak form keeps the term $\int_{\Gamma_D} v \nabla u \cdot \mathbf{n} \, d\Gamma$ from the consistent weak form (44), and includes new terms maintaining the consistency.*

The only problem of Nitsche's method is the deduction of the weak form. The generalization of the implementation for other problems is not as straightforward as for the method of Lagrange multipliers or for the penalty method. The weak form and the choice of parameter β depends not only on the partial differential equation, but also on the essential boundary condition to be prescribed. Nitsche's method applied to other problems is discussed by Nitsche

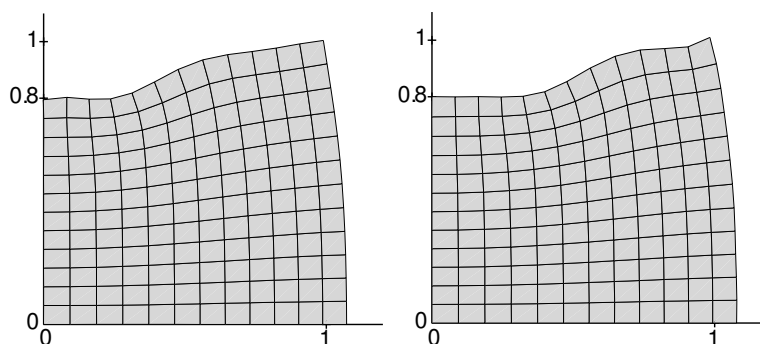


Figure 13. Nitsche's solution, 7×7 distribution of particles, for $\beta = 100$ (left) and $\beta = 10^4$ (right)

(1970), by Becker (2002) for the Navier-Stokes problem, by Freud and Stenberg (1995) for the Stokes problem, by Hansbo and Larson (2002) for elasticity problems.

Regarding the choice of the parameter, Nitsche proved that if β is taken as $\beta = \alpha/h$, where α is a large enough constant and h denotes the characteristic discretization measure, then the discrete solution converges to the exact solution with optimal order in \mathcal{H}^1 and \mathcal{L}^2 norms. Moreover, for model problem (43) with Dirichlet boundary conditions, $\Gamma_D = \partial\Omega$, a value for constant α can be determined taking into account that convergence is ensured if $\beta > 2C^2$, where C is a positive constant such that $\|\nabla v \cdot \mathbf{n}\|_{\mathcal{L}^2(\partial\Omega)} \leq C\|\nabla v\|_{\mathcal{L}^2(\Omega)}$ for all v in the chosen interpolation space. This condition ensures the coercivity of the bilinear form in the interpolation space. Griebel and Schweitzer (2002) propose the estimation of the constant C as the maximum eigenvalue of the generalized eigenvalue problem,

$$\mathbf{A}\mathbf{v} = \lambda\mathbf{B}\mathbf{v}, \quad (58)$$

where

$$A_{ij} = \int_{\partial\Omega} (\nabla N_i \cdot \mathbf{n})(\nabla N_j \cdot \mathbf{n}) \, d\Gamma, \quad B_{ij} = \int_{\Omega} \nabla N_i \cdot \nabla N_j \, d\Omega.$$

The problem described in Figure 9 can be solved by Nitsche's method for different values of β , see Figure 13. Note that the modification of the weak form is not trivial in this case, see Fernández-Méndez and Huerta (2004). The major advantage of Nitsche's method is that scalar parameter β need not be as large as in the penalty method, and avoids to meet the LBB condition for the interpolation space for the Lagrange multiplier.

3.4. Incompressibility and volumetric locking in mesh-free methods

Locking in finite elements has been a major concern since its early developments. It appears because poor numerical interpolation leads to an over-constrained system. Locking of standard finite elements has been extensively studied. It is well known that bilinear finite elements lock in some problems and that biquadratic elements have a better behavior (Hughes, 2000). Moreover, locking has also been studied for increasing polynomial degrees in the context of an hp adaptive strategy, see Suri (1996).

In fact, *locking* is used in the context of solid mechanics. It is a concern for nearly incompressible materials. Recall that in plasticity the material is incompressible (Belytschko

et al., 2000). For instance, let's consider a linear elastic isotropic material under plane strain conditions and small deformations, namely $\nabla^s \mathbf{u}$, where \mathbf{u} is the displacement and ∇^s the symmetric gradient, *i.e.* $\nabla^s = \frac{1}{2}(\nabla^T + \nabla)$. Dirichlet boundary conditions are imposed on Γ_D , a traction \mathbf{h} is prescribed along the Neumann boundary Γ_N and there is a body force \mathbf{f} . Thus, the problem that needs to be solved may be stated as: solve for $\mathbf{u} \in [\mathcal{H}_{\Gamma_D}^1]^2$ such that

$$\begin{aligned} \frac{E}{1+\nu} \int_{\Omega} \nabla^s \mathbf{v} : \nabla^s \mathbf{u} \, d\Omega + \frac{E\nu}{(1+\nu)(1-2\nu)} \int_{\Omega} (\nabla \cdot \mathbf{v})(\nabla \cdot \mathbf{u}) \, d\Omega \\ = \int_{\Omega} \mathbf{f} \cdot \mathbf{v} \, d\Omega + \int_{\Gamma_N} \mathbf{h} \cdot \mathbf{v} \, d\Gamma \quad \forall \mathbf{v} \in [\mathcal{H}_{0,\Gamma_D}^1]^2. \end{aligned} \quad (59)$$

In this equation, the standard vector subspaces of \mathcal{H}^1 are employed for the solution \mathbf{u} , $[\mathcal{H}_{\Gamma_D}^1]^2 := \{\mathbf{u} \in [\mathcal{H}^1]^2 \mid \mathbf{u} = \mathbf{u}_D \text{ on } \Gamma_D\}$ (Dirichlet conditions, \mathbf{u}_D , are automatically satisfied) and for the test functions \mathbf{v} , $[\mathcal{H}_{0,\Gamma_D}^1]^2 := \{\mathbf{v} \in [\mathcal{H}^1]^2 \mid \mathbf{v} = \mathbf{0} \text{ on } \Gamma_D\}$, (zero values are imposed along Γ_D).

This equation, as discussed by Suri (1996), shows the inherent difficulties of the incompressible limit. The standard *a priori* error estimate emanating from (59) and based on the energy norm may become unbounded for values of ν close to 0.5. In fact, in order to have finite values of the energy norm the divergence-free condition must be enforced in the continuum case, *i.e.* $\nabla \cdot \mathbf{u} = 0$ for $\mathbf{u} \in [\mathcal{H}_{\Gamma_D}^1]^2$, and also in the finite approximation dimensional space. In fact, locking will occur when the approximation space is not rich enough for the approximation to verify the divergence-free condition.

In fluids, the *incompressibility* is directly the concern. Accurate and efficient modelling of incompressible flows is an important issue in finite elements. The continuity equation for an incompressible fluid takes a peculiar form. It consists of a constraint on the velocity field which must be divergence free. Then, the pressure has to be considered as a variable not related to any constitutive equation. Its presence in the momentum equation has the purpose of introducing an additional degree of freedom needed to satisfy the incompressibility constraint. The role of the pressure variable is thus to adjust itself instantaneously in order to satisfy the condition of divergence-free velocity. That is, the pressure is acting as a Lagrange multiplier of the incompressibility constraint and thus there is a coupling between the velocity and the pressure unknowns.

Various formulations have been proposed for incompressible flow (Girault and Raviart, 1986; Gresho and Sani, 2000; Gunzburger, 1989; Pironneau, 1989; Quartapelle, 1993; Quarteroni and Valli, 1994; Temam, 2001; Donea and Huerta, 2003). Mixed finite elements present numerical difficulties caused by the saddle-point nature of the resulting variational problem. Solvability of the problem depends on a proper choice of finite element spaces for velocity and pressure. They must satisfy a compatibility condition, the so-called LBB (or inf-sup) condition. If this is not the case, alternative formulations (usually depending on a numerical parameter) are devised to circumvent the LBB condition and enable the use of velocity–pressure pairs that are unstable in the standard Galerkin formulation.

Incompressibility in mesh-free methods is still an open topic. Even recently, it was claimed (Zhu and Atluri, 1998) that meshless methods do not exhibit volumetric locking. Now it is clear that this is not true, as shown in a study of the element free Galerkin (EFG) method by Dolbow and Belytschko (1999). Moreover, several authors claim that increasing the dilation parameter locking phenomena in mesh-free methods can be suppressed, or at least attenuated

(Askes *et al.*, 1999; Dolbow and Belytschko, 1999; Chen *et al.*, 2000). Huerta and Fernández-Méndez (2001) clarify this issue and determine the influence of the dilation parameter on the locking behavior of EFG near the incompressible limit by a modal analysis. The major conclusions are:

- 1.- The number of non-physical locking modes is independent of the ratio ρ/h .
- 2.- An increase of the dilation parameter decreases the eigenvalue (amount of energy) in the locking mode and attenuates, but does not suppress volumetric locking (in the incompressible limit the energy will remain unbounded).
- 3.- An increase in the order of consistency decreases the number of non-physical locking modes.
- 4.- The decrease in the number of non-physical locking modes is slower than in finite elements. Thus EFG will not improve the properties of the FEM (from a volumetric locking viewpoint) for p or h - p refinement. However, for practical purposes and as in finite elements, in EFG an h - p strategy will also suppress locking.

The remedies proposed in the literature are, in general, extensions of the methods developed for finite elements. For instance, Dolbow and Belytschko (1999) propose an EFG formulation using selective reduced integration. Chen *et al.* (2000) suggest an improved RKPM based on a pressure projection method. These alternatives have the same advantages and inconveniences as in standard finite element methods. Perhaps it is worth noting that in mesh-free methods it is non trivial to verify analytically the LBB condition for a given interpolation of velocity and pressure.

One alternative that uses the inherent properties of mesh-free methods and does not have a parallel in finite elements is the pseudo-divergence-free approach (Vidal *et al.*, 2002; Huerta *et al.*, 2004a). This method is based on diffuse derivatives (see Section 2.2.6) which converge to the derivatives of the exact solution when the radius of the support, ρ , goes to zero (for a fixed ratio ρ/h). One of the key advantages of this approach is that the expressions of pseudo-divergence-free interpolation functions are computed *a priori*. That is, prior to determining the specific particle distribution. Thus, there is no extra computational cost because only the interpolating polynomials are modified compared with standard EFG.

4. RADIAL BASIS FUNCTIONS

Radial basis functions (RBF) have been studied in mathematics for the past 30 years and are closely related to mesh-free approximations. There are two major differences in between the current practice approaches in radial basis functions and those described in previous Sections:

1. Most radial basis functions have non compact support.
2. Completeness is provided by adding a global polynomial to the basis.

For these two reasons, the solution procedures usually have to be tailored for this class of global interpolants. Two techniques that avoid the drawbacks of global approximations are

1. Multipolar methods
2. Domain decomposition techniques

The most commonly used radial basis functions (with their names) are

$$\Phi_I(\mathbf{x}) = \begin{cases} \|\mathbf{x} - \mathbf{x}_I\| \equiv r & \text{linear} \\ r^2 \log r & \text{thin plate spline} \\ e^{-r^2/c^2} & \text{Gaussian} \\ (r^2 + R^2)^q & \text{multipolar} \end{cases}$$

where c , R and q are shape parameters. The choice of these shape parameters has been studied by Kansa and Carlsson (1992), Carlsson and Foley (1991) and Rippa (1999).

Completeness of the radial basis function approximations is usually provided by adding a global polynomial to the approximation. For example, an approximation with quadratic completeness, is

$$u(\mathbf{x}) = c_0 + \sum_{i=1}^{n_{sd}} c_j x_j + \sum_{i=1}^{n_{sd}} \sum_{j=1}^{n_{sd}} d_{ij} x_i x_j + \sum_I a_I \Phi(\mathbf{x}_I)$$

where c_0 , c_j , d_{ij} and a_I are the unknown parameters.

One of the major applications of Radial basis functions has been in data fitting. The reference by Carr *et al.* (1997), where millions of data points are fit, is illustrative of the power of this method. One of the first applications to the solution of PDEs is given by Kansa (1990), who used multiquadrics for smooth problems in fluid dynamics. In Sharan *et al.* (1997), the method was applied to elliptic PDE's. In both cases, collocation was employed for the discretization. Exceptional accuracy was reported. Although a global understanding of this behavior is not yet available, evidently very smooth global approximants have intrinsic advantages over rough approximants for elliptic PDEs and other smooth problems (any locally supported approximant will have some roughness at the edge of its support). The low cost of RBF evaluation is another advantage. Wendland (1999) has studied Galerkin discretization of PDEs with radial basis functions. Compactly supported RBFs are also under development. Local error estimates for radial basis approximations of scattered data are given by Wu and Schaback (1993).

5. DISCONTINUITIES

One of the most attractive attributes of mesh-free methods is their effectiveness in the treatment of discontinuities. This feature is particularly useful in solid mechanics in modelling cracks and shear bands.

The earliest methods for constructing discontinuous mesh-free approximations were based on the visibility criterion Organ *et al.* (1996). In this method, in constructing the approximation at \mathbf{x} , the nodes on the opposite side of the discontinuity are excluded from the index set S_x^p , i.e. nodes on the opposite side of the discontinuity do not effect the approximation at \mathbf{x} . To be more precise, if the discontinuity is described implicitly (i.e. by a level set) by $f(\mathbf{x}) = 0$, with $f(\mathbf{x}) > 0$ on one side, $f(\mathbf{x}) < 0$ on the other, then

$$\begin{cases} f(\mathbf{x}_I) f(\mathbf{x}) > 0 & \Rightarrow I \in S_x^p, \\ f(\mathbf{x}_I) f(\mathbf{x}) < 0 & \Rightarrow I \notin S_x^p. \end{cases}$$

The name ‘‘visibility’’ criterion originates from the notion of considering a discontinuity as an opaque surface while choosing the nodes that influence the approximation at a point \mathbf{x} ,

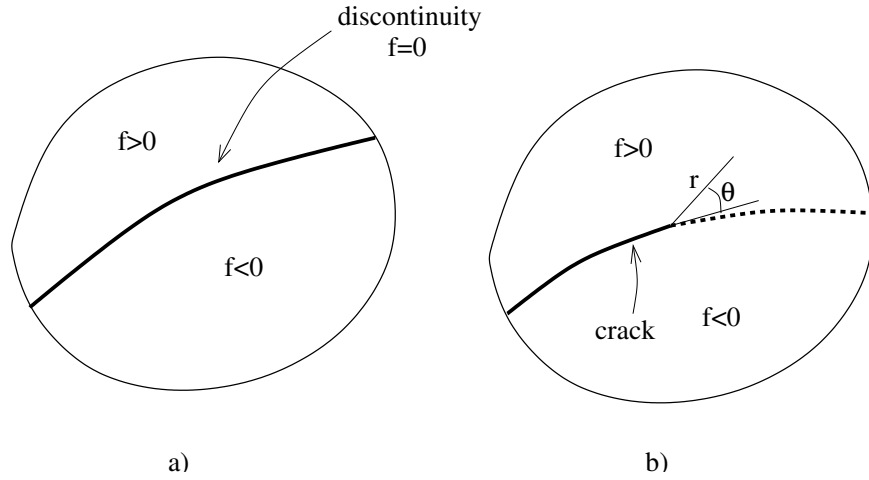


Figure 14. a) level set describing discontinuity, b) nomenclature for cracktip branch functions

namely S_x^p . If a node \mathbf{x}_I is invisible from \mathbf{x} , then node I is not included in the index set S_x^p even when it falls within the domain of influence.

When a discontinuity ends within a domain, such as at a cracktip, the visibility criterion does not provide an adequate tool for constructing the discontinuity in the approximation. Around the cracktip the approximation must be constructed so that it is continuous in front of the cracktip, but discontinuous behind it. One way to accomplish this is to include in the basis branch functions of the form

$$B_{iI} = [r^2 \sin \frac{\theta}{2}, r^2 \sin \frac{\theta}{2}] \quad (60)$$

where θ is the angle between the line to the cracktip and the tangent to the crack and r is the distance to the cracktip, see Fig. 14b.

For cracks in elastic materials, the basis can be enriched by branch functions that span the asymptotic neartip field of the Westergard solution, see Fleming *et al.* (1997). The basis is then the polynomial basis plus the functions

$$B_{iI} = [\sqrt{r} \sin \frac{\theta}{2}, \sqrt{r} \sin \frac{\theta}{2} \sin \theta, \sqrt{r} \cos \frac{\theta}{2}, \sqrt{r} \cos \frac{\theta}{2} \cos \theta] \quad (61)$$

Since this basis includes the first order terms in the neartip field solution, very accurate solutions can be obtained with coarse discretizations. Xiao and Karihaloo (2003) have shown that even better accuracy can be attained by adding higher order terms in the asymptotic field. The idea of incorporating special functions can also be found, among others, in Oden and Duarte (1997).

Regardless of whether a branch function is used near the cracktip, if the visibility criterion is used for constructing the approximation near the end of the discontinuity, additional discontinuities may occur around the tip. Two such discontinuities are shown in Fig. 15. They can be avoided if the visibility criterion is not used near the tip. Krysl and Belytschko (1997) have shown that these discontinuities do not impair the convergence of the solution since their

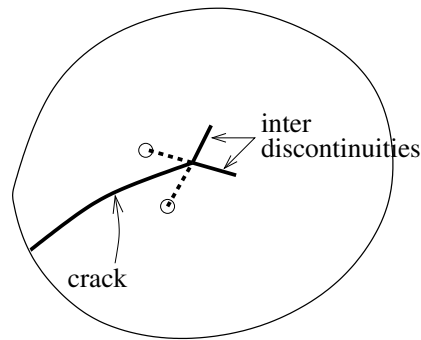


Figure 15. Inter discontinuity in visibility criterion method

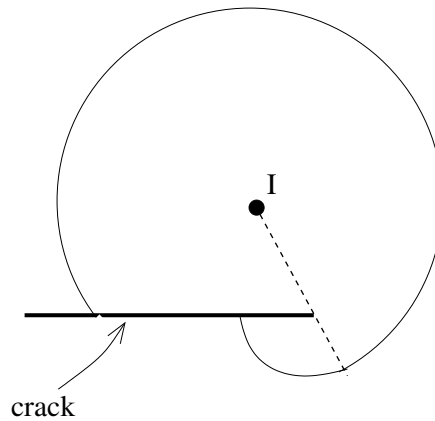


Figure 16. Domain of influence of node I by the transparency method near the crack tip

length, and hence the energy of the discontinuity, decreases with h . However, these extraneous discontinuities complicate the integration of the weak form, so several techniques have been developed to smooth the approximation around the tip of a discontinuity; the diffraction and the transparency method.

In the transparency method, the crack near the crack tip is made transparent. The degree of transparency is related to the distance from the crack tip to the point of intersection. The shape functions are smoothed around the crack tip as shown in Fig. 16. The diffraction method is similar to the transparency method. The shape function is smoothed similar to the way light diffracts around a corner.

The recommended technique for including discontinuities is based on the partition of unity property of the approximants. It was first developed in the context of the extended finite element method, Moes *et al.* (1999), Belytschko and Black (1999) and Dolbow *et al.* (2000). It was applied in EFG by Ventura *et al.* (2002). Let the set of particles whose support is intersected by the discontinuity be denoted by S^D , and the set of particles whose support

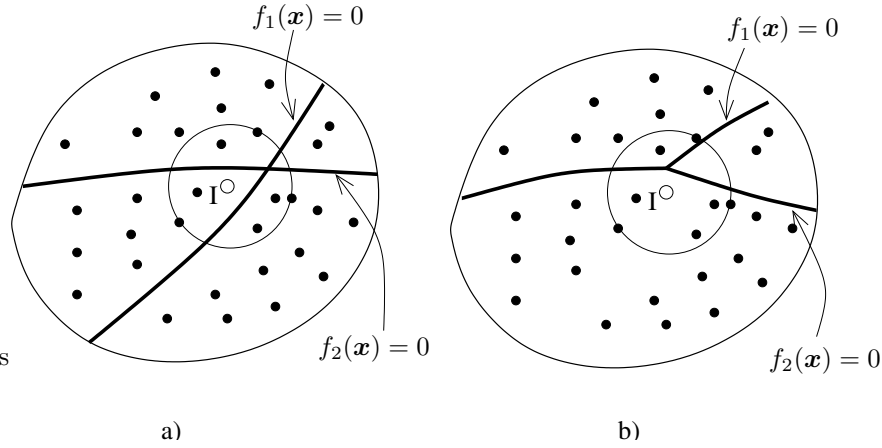


Figure 17. a) Support of node I with a) intersecting discontinuities and b) branching discontinuities

includes the tip of the discontinuity by S^T . The approximation is then given by

$$\mathbf{u}^h(\mathbf{x}) = \sum_{I \in S_x^p} N_I(\mathbf{x}) \mathbf{u}_I + \sum_{I \in S^D \cap S_x^p} N_I(\mathbf{x}) H(f(\mathbf{x})) \mathbf{q}_I^{(1)} + \sum_{I \in S^T \cap S_x^p} N_I(\mathbf{x}) \sum_J \left(\mathbf{B}_J \cdot \mathbf{q}_J^{(2)} \right),$$

where $H(\cdot)$ is the step function (Heaviside function). It is easy to show that the weak form (see Belytschko and Black, 1999) then yields the requisite strong form for elastic problems; this is probably also true for partial differential equations describing other physical problems.

The technique can also be used for intersecting and branching discontinuities, see Daux *et al.* (2000) and Belytschko *et al.* (2001). For example, consider the geometry shown in Fig. 17. Let J^1 be the set of nodes whose domains of influence include the discontinuity $f_1(\mathbf{x}) = 0$, J^2 the corresponding set for $f_2(\mathbf{x}) = 0$. Let $J^3 = J^1 \cap J^2$. Then the approximation is

$$\begin{aligned} \mathbf{u}^h(\mathbf{x}) = & \sum_{I \in S_x^p} N_I(\mathbf{x}) \mathbf{u}_I + \sum_{I \in J^1 \cap S_x^p} N_I(\mathbf{x}) H(f_1(\mathbf{x})) \mathbf{q}_I^{(1)} \\ & + \sum_{I \in J^2 \cap S_x^p} N_I(\mathbf{x}) H(f_2(\mathbf{x})) \mathbf{q}_I^{(2)} + \sum_{I \in J^3 \cap S_x^p} N_I(\mathbf{x}) H(f_1(\mathbf{x})) H(f_2(\mathbf{x})) \mathbf{q}_I^{(3)}. \end{aligned}$$

5.1. Discontinuities in gradients

The continuously differentiable character of mesh-free approximation functions is sometimes a disadvantage. At material interfaces in continua, or more generally, at discontinuities of the coefficients of a PDE, solutions of elliptic and parabolic systems have discontinuous gradients. These discontinuities in the gradient need to be explicitly incorporated in mesh-free methods.

One of the first treatments of discontinuous gradients was by Cordes and Moran (1996). They treated the construction of the approximation separately; that is, they subdivided the domain into two subdomains. Let the subdomains Ω_1 and Ω_2 be with interface Γ^{int} . They enforced continuity of the function along Γ^{int} by Lagrange multipliers. Since the approximation $u(\Omega_1)$ was constructed without considering any nodes in Ω_2 , and vice versa, the gradient of

the approximation will be discontinuous across Γ^{int} after the continuity of the approximation is enforced by Lagrange multipliers. As in the case of essential boundary conditions, this continuity of the function can also be enforced by penalty methods, augmented Lagrangian methods or Nitsche's method.

An alternative technique was proposed by Krongauz and Belytschko (1998a), who added a function with a discontinuous gradient. In the original paper, the approximation is enriched with the absolute values of a signed distance function.

This enrichment function can also be employed with a local or global partition of unity

$$u^h = N_i u_i + N_i |f(\mathbf{x})| q_i$$

This was first studied in a finite element context by Sukumar *et al.* (2001) and Belytschko *et al.* (2001). In a finite element, the local partition of unity has some difficulties because the enrichment function does not decay, so it is difficult to fade it out gracefully. A global partition of unity is also undesirable. This behavior of this enrichment in mesh-free methods has not been studied.

The local partition of unity method can also be used for intersecting gradient discontinuities, branching gradient discontinuities and unclosed gradient discontinuities. The techniques are identical to those for discontinuities in functions, except that the step function is replaced by the absolute values of the signed distance function. For example, the approximation for a function with the intersecting discontinuities shown in Fig. 17a is given by

$$\begin{aligned} u^h(\mathbf{x}) = & \sum_{I \in S_1^g} N_I(\mathbf{x}) u_I + \sum_{I \in J^1 \cap S_1^g} N_I(\mathbf{x}) |f_1(\mathbf{x})| \mathbf{q}_I^{(1)} \\ & + \sum_{I \in J^2 \cap S_1^g} N_I(\mathbf{x}) |f_2(\mathbf{x})| \mathbf{q}_I^{(2)} + \sum_{I \in J^3 \cap S_1^g} N_I(\mathbf{x}) |f_1(\mathbf{x})| |f_2(\mathbf{x})| \mathbf{q}_I^{(3)}. \end{aligned}$$

The enrichment procedures are substantially simpler to implement than the domain subdivision/constraint technique of Cordes and Moran (1996), particularly for complex patterns such as intersecting and branching gradient discontinuities.

6. BLENDING MESH-FREE METHODS AND FINITE ELEMENTS

Several authors have proposed different alternatives to blend finite elements and mesh-free methods. These approximations are combined for two purposes: either *i*) to couple both interpolations, or *ii*) to enrich the finite element interpolation using particles.

In the first scenario, the objective is to benefit from the advantages of each interpolation in different regions of the computational domain, which is usually divided in three regions, see Figure 18. In one region only finite elements are present, another with only mesh-free approximation functions, and a transition region.

In the second case, the enrichment improves the approximation without remeshing. A finite element interpolation is considered in the whole domain and particles can be added in order to improve the interpolation in a selected region.

Coupled finite elements/mesh-free methods are proposed by Belytschko *et al.* (1995). They show how to couple finite elements near the Dirichlet boundaries and EFG in the interior of

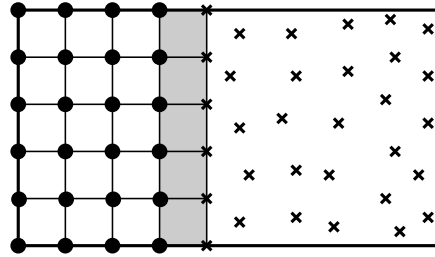


Figure 18. Discretization for the coupling of finite elements and a mesh-free method: finite element nodes (•), particles (x) and transition region (in gray).

the computational domain. This simplifies considerably the prescription of essential boundary conditions. The mixed interpolation in the transition region requires the substitution of finite element nodes by particles and the definition of ramp functions. Thus the region for transition is of the size of one finite element (as in Figure 18) and the interpolation is linear. With the same objectives Hegen (1996) couples the finite element domain and the mesh-free region with Lagrange multipliers.

Liu *et al.* (1997b) independently suggest to enrich the finite element approximation with particle methods. In fact, the following adaptive process seems attractive: (1) compute an approximation with a coarse finite element mesh, (2) do an *a posteriori* error estimation and (3) improve the solution with particles without any remeshing process.

Following these ideas, Huerta and Fernández-Méndez (2000) propose a unified and general formulation: the continuous blending method. This formulation allows both coupling and enrichment of finite elements with mesh-free methods. The continuous blending method generalizes the previous ideas for any order of approximation, suppresses the ramp functions, and it does not require the substitution of nodes by particles. That is, as many particles as needed can be added where they are needed, independently of the adjacent finite element mesh. This is done in a hierarchical manner. This approach has been generalized in Chen *et al.* (2003) to get a nodal interpolation property.

Other alternatives are also possible; for instance, the bridging scale method proposed by Wagner and Liu (2000) is a general technique to mix a mesh-free approximation with any other interpolation space, in particular with finite elements. Huerta *et al.* (2004b) compare the continuous blending method and the bridging scale method, for the implementation of essential boundary conditions. The bridging scale method does not vanish between the nodes along the essential boundary. As noted by Wagner and Liu (2000) a modified weak form must be used to impose the essential boundary condition and avoid a decrease in the rate of convergence.

Next section is devoted to the continuous blending method proposed by Huerta and Fernández-Méndez (2000). This method allows to recall the basic concepts on both enrichment and coupling. Although all the developments are done for the EFG method, the continuous blending method is easily generalizable to other mesh-free methods based on an MLS approximation.

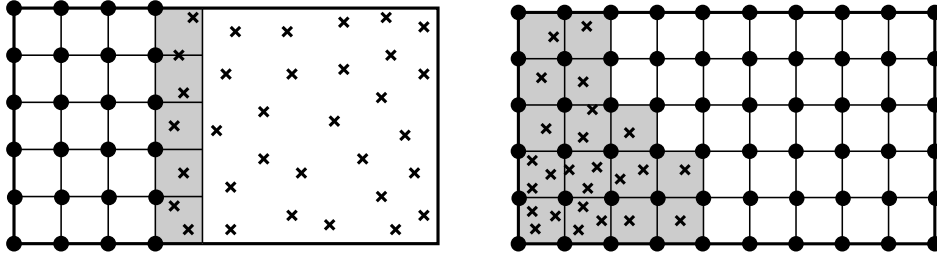


Figure 19. Possible discretizations for the continuous blending method

6.1. Continuous blending method

Huerta and coworkers (Huerta and Fernández-Méndez, 2000; Fernández-Méndez and Huerta, 2002; Fernández-Méndez *et al.*, 2003) propose a continuous blending of EFG and finite element methods,

$$u(\mathbf{x}) \simeq \tilde{u}(\mathbf{x}) = \sum_{j \in \mathcal{J}} N_j^h(\mathbf{x}) u_j + \sum_{i \in \mathcal{I}} \tilde{N}_i^\rho(\mathbf{x}) u_i = \mathcal{P}^h u + \sum_{i \in \mathcal{I}} \tilde{N}_i^\rho(\mathbf{x}) u_i \quad (62)$$

where the finite element shape functions $\{N_j^h\}_{j \in \mathcal{J}}$ are as usual, and the mesh-free shape functions $\{\tilde{N}_i^\rho\}_{i \in \mathcal{I}}$ take care of the required consistency of the approximation, i.e. consistency of order m . \mathcal{P}^h denotes the projection operator onto the finite element space. Figure 19 presents two examples for the discretization. Particles are marked with \times and *active nodes*, $\{\mathbf{x}_j\}_{j \in \mathcal{J}}$ for the functional interpolation, are marked with \bullet . Other *non-active nodes* are considered to define the support of the finite element shape functions (thus only associated to the geometrical interpolation). The first discretization (left) can be used for the coupling situation. Note that with the continuous blending method the particles can be located where they are needed independently of the adjacent finite element mesh. In the second one (right) a finite element mesh is considered in the whole domain and particles are added to enrich the interpolation, and increase the order of consistency, in the gray region.

The mesh-free shape functions required in (62) are defined as in standard EFG, see equation (28),

$$\tilde{N}_i^\rho(\mathbf{x}) = \omega(\mathbf{x}_i, \mathbf{x}) \mathbf{P}^\top(\mathbf{x}_i) \tilde{\boldsymbol{\alpha}}(\mathbf{x}), \quad (63)$$

but now the unknown vector $\tilde{\boldsymbol{\alpha}}$ is determined by imposing the reproducibility condition associated to the combined EFG and finite element approximation, that is

$$\mathbf{P}(\mathbf{x}) = \mathcal{P}^h \mathbf{P}(\mathbf{x}) + \sum_{i \in \mathcal{I}} \tilde{N}_i^\rho(\mathbf{x}) \mathbf{P}(\mathbf{x}_i). \quad (64)$$

Substitution of (63) in (64) leads to a small system of equations for $\tilde{\boldsymbol{\alpha}} \in \mathbb{R}^{l+1}$, see Huerta and Fernández-Méndez (2000) for details,

$$\mathbf{M}(\mathbf{x}) \tilde{\boldsymbol{\alpha}}(\mathbf{x}) = \mathbf{P}(\mathbf{x}) - \mathcal{P}^h \mathbf{P}(\mathbf{x}). \quad (65)$$

The only difference with standard EFG is the modification of the r.h.s. of the previous system, in order to take into account the contribution of the finite element base in the

approximation. Moreover, note that the expression for the modified EFG shape functions is independent of the situation, i.e the same implementation is valid for enrichment and coupling, increasing the versatility of this approach.

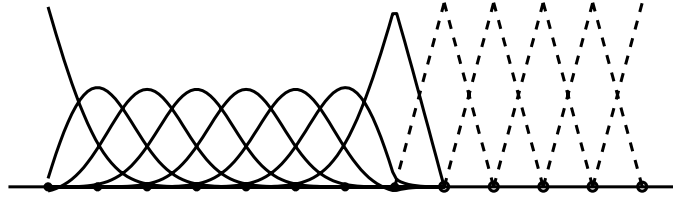


Figure 20. Shape functions of the coupled finite element (solid line) and mesh-free (dashed line) interpolation.

Figure 20 shows a 1D example coupling finite elements and EFG. The mesh-free shape functions adapt their shape to recover the linear interpolation. In the coupling situation the continuity of the interpolation is ensured under some conditions, even in multiple dimensions, by the following result, see Fernández-Méndez and Huerta (2002; 2004) for the proof.

Proposition 3. *The approximation $\tilde{u}(x)$, defined in (62), is continuous in Ω if: (1.-) the same order of consistency, m , is imposed all over Ω (i.e. m coincides with the degree of the FE base), and (2.-) the domain of influence of particles coincides exactly with the region where finite elements do not have a complete basis.*

Remark 24 (Imposing Dirichlet boundary conditions) *Under the assumptions (1.-) and (2.-) in **Proposition 3**, the contribution of the particles is zero in the regions where the finite element base is complete. In particular, this means that $\tilde{N}_i^p = 0$ in the finite element edges (or faces in 3D) whose nodes are all in \mathcal{J} (active nodes). This is an important property for the implementation of essential boundary conditions. If a finite element mesh with active nodes at the essential boundary is used, the mesh-free shape functions take care of reproducing polynomials up to degree m in Ω and, at the same time, vanish at the essential boundary. For instance, Figure 21 shows the particle shape functions, $\tilde{N}_i^p = 0$, associated to particles at the boundary and in the first interior layer. Note that they vanish along the boundary because the finite element base is complete on $\partial\Omega$. Therefore, the prescribed values can be directly imposed as usual in the framework of finite elements, by setting the values of the corresponding nodal coefficients. Moreover, it is also easy to impose that the test functions (for the weak forms) vanish along the Dirichlet boundary, see Fernández-Méndez and Huerta (2004) for further details.*

The problem described in Figure 9 can be solved using the continuous blending method, Figure 22 shows the solution. As observed in Remark 24, the prescribed displacements are directly imposed. Two different finite element discretizations are considered. In both cases, the linear finite element approximation at the boundary, allows the exact enforcement of the prescribed displacement. Note that if the prescribed displacement is piecewise linear or piecewise constant, as it is in this example, then it is imposed exactly when a bilinear finite element approximation is used.

Finally, an example reproduces the finite element enrichment with EFG in a nonlinear computational problem. A rectangular specimen with an imperfection is loaded (see Díez *et*

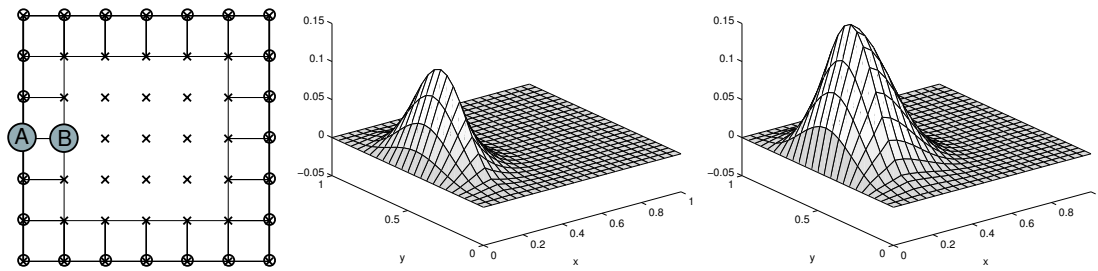


Figure 21. Discretization with active finite element nodes at the boundary (o) and particles (x), and mesh-free shape function associated to the particle located at the gray circle (A) and (B) respectively.

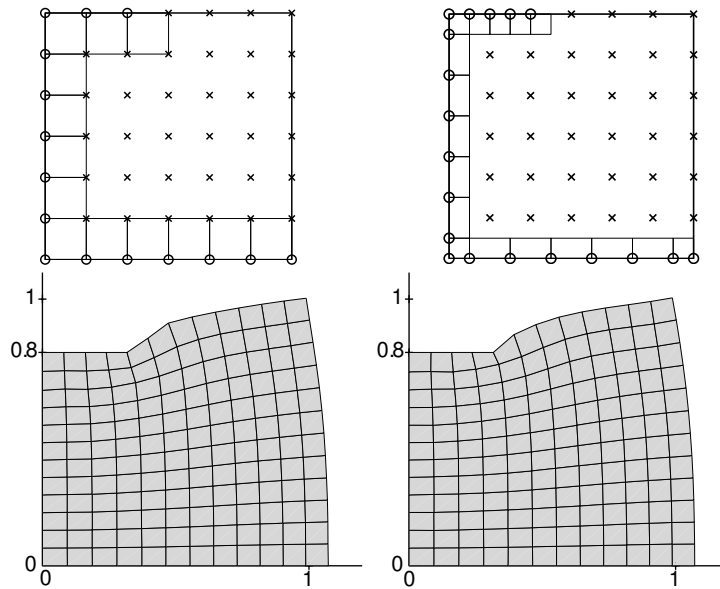


Figure 22. Continuous blending for two different distributions of finite elements near the essential boundary and the same distribution of particles, $h = 1/6$

al., 2000; Huerta and Díez, 2000). Figure 23 presents the problem statement with the material properties.

This problem has been solved with the element free Galerkin method. A coarse mesh solution of quadrilateral bilinear finite elements (308 dof) is shown in Figure 25 (left). When particles are added ($308+906=1214$ dof) and the order of consistency is increased ($m = 2$), an accurate distribution of inelastic strains is recovered, see Figure 25.

In this example, Figure 25, the original mesh is maintained and particles are added where they are needed.

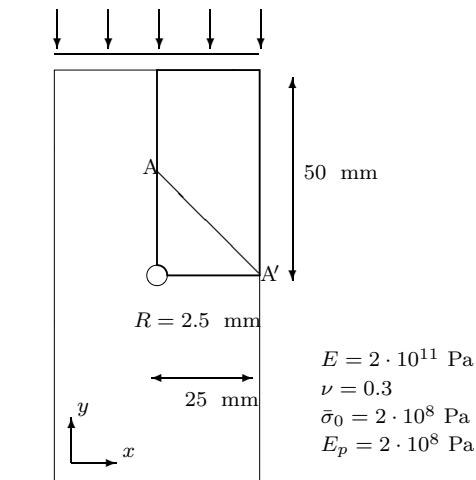


Figure 23. Problem statement: rectangular specimen with one centered imperfection.

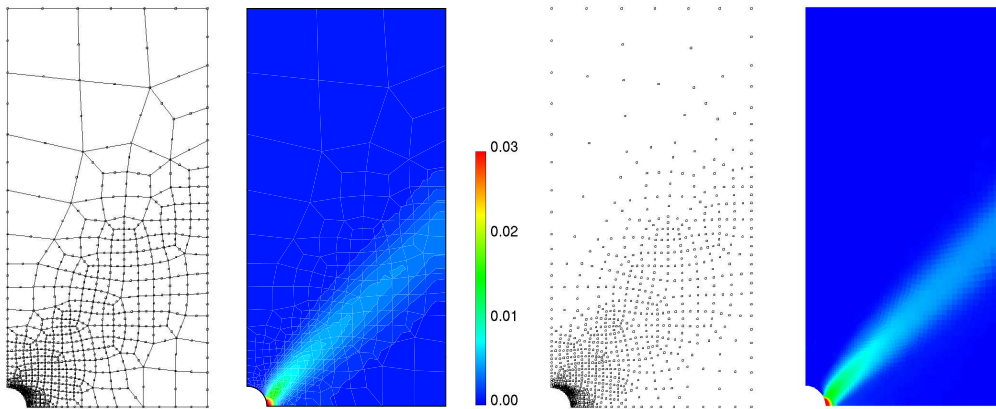


Figure 24. Final mesh with its corresponding equivalent inelastic strain for a standard finite element (8 noded elements) computation (left) and distribution of particles with its inelastic strain distribution for EFG (right).

REFERENCES

- Aluru N. A point collocation method based on reproducing kernel approximations. *Int. J. Numer. Methods Eng.*, **47**(6):1083–1121, 2000.
- Arnold DN, Brezzi F, Cockburn B and Marini LD. Unified analysis of discontinuous Galerkin methods for elliptic problems. *SIAM J. Numer. Anal.*, **39**(5):1749–1779, 2001/02.
- Askes H, de Borst R and Heeres O. Conditions for locking-free elasto-plastic analyses in the element-free Galerkin method. *Comput. Methods Appl. Mech. Eng.*, **173**(1–2):99–109, 1999.

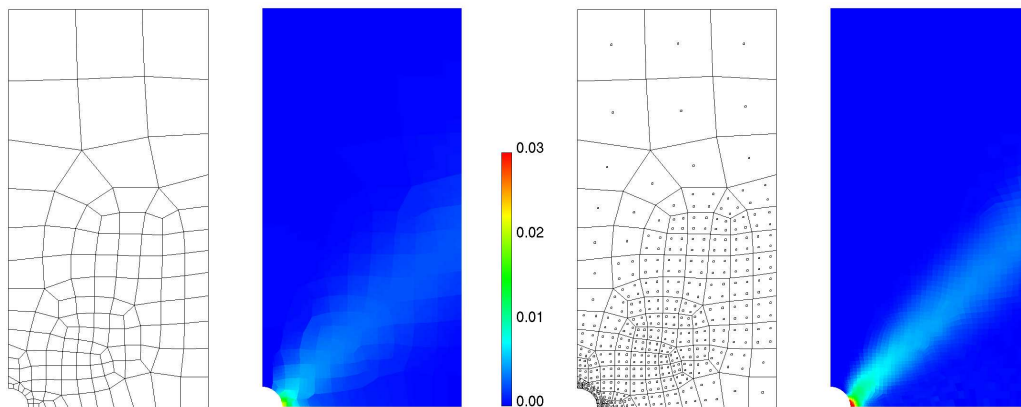


Figure 25. Coarse finite element mesh (Q1 elements) with its corresponding equivalent inelastic strain (right) and mixed interpolation with its equivalent inelastic strain distribution (left).

Babuška I and Melenk J. The partition of the unity finite element method. Technical Report BN-1185, Institute for Physical Science and Technology, University of Maryland, Maryland, 1995.

Babuska I, Banerjee U and Osborn JE. Meshless and generalized finite element methods: A survey of some major results. In Griebel M and Schweitzer MA, editors, *Meshfree methods for partial differential equations*, volume 26 of *Lecture Notes in Computational Science and Engineering*, pages 1–20. Springer-Verlag, Berlin, 2002.

Babuska I. The finite element method with lagrange multipliers. *Numer. Math.*, **20**:179–192, 1973.

Babuska I. The finite element method with penalty. *Math. Comp.*, **27**:221–228, 1973.

Becker R. Mesh adaptation for dirichlet flow control via Nitsche’s method. *Commun. Numer. Methods Eng.*, **18**(9):669–680, 2002.

Belytschko T and Black T. Elastic crack growth in finite elements with minimal remeshing. *Int. J. Numer. Methods Eng.*, **45**(5):601–620, 1999.

Belytschko T and Organ D. Element-free Galerkin methods for dynamic fracture in concrete. In D.R.J. Owen EO and Hilton E, editors, *Computational Plasticity. Fundamentals and Applications*, pages 304–321, Barcelona, Spain, 1997.

Belytschko T, Lu YY and Gu L. Element free Galerkin methods. *Int. J. Numer. Methods Eng.*, **37**(2):229–256, 1994.

Belytschko T, Organ D and Krongauz Y. A coupled finite element–element-free Galerkin method. *Comput. Mech.*, **17**(3):186–195, 1995.

Belytschko T, Krongauz Y, Organ D, Fleming M and Krysl P. Meshless methods: an overview and recent developments. *Comput. Methods Appl. Mech. Eng.*, **139**(1–4):3–47, 1996.

Belytschko T, Krongauz Y, Fleming M, Organ D and Liu WK. Smoothing and accelerated computations in the element free Galerkin method. *J. Comput. Appl. Math.*, **74**(1–2):111–126, 1996.

- Belytschko T, Liu WK and Moran B. *Nonlinear finite elements for continua and structures*. John Wiley & Sons, Chichester, 2000.
- Belytschko T, Moes N, Usui S and Parimi C. Arbitrary discontinuities in finite elements. *Int. J. Numer. Methods Eng.*, **50**(4):993–1013, 2001.
- Bonet J and Kulasegaram S. Correction and stabilization of smooth particle hydrodynamics methods with applications in metal forming simulations. *Int. J. Numer. Methods Eng.*, **47**(6):1189–1214, 2000.
- Bonet J and Lok T. Variational and momentum preservation aspects of smooth particle hydrodynamic formulations. *Comput. Methods Appl. Mech. Eng.*, **180**(1-2):97–115, 1999.
- Bouillard P and Suleau S. Element-free Galerkin method for helmholtz problems: formulation and numerical assessment of the pollution effect. *Comput. Methods Appl. Mech. Eng.*, **162**(1-4):317–335, 1998.
- Breitkopf P, Rassineux A and Villon P. Mesh-free operators for consistent field transfer in large deformation plasticity. In *Book of abstracts of the 2nd European Conference on Computational Mechanics: Solids, Structures and Coupled Problems in Engineering*, Cracow, Poland, 2001.
- Brezzi F. On the existence, uniqueness and approximation of saddle-point problems arising from Lagrangian multipliers. *Rev. Française Automat. Informat. Recherche Opérationnelle Sér. Rouge*, **8**(R-2):129–151, 1974.
- Carlsson R and Foley T. The parameter r^2 in multiquadric interpolation. *Computers and Mathematics with applications*, **21**:29–42, 1991.
- Carr JC, Fright WR and Beatson RK. Surface interpolation with radial basis functions for medical imaging. *IEEE Trans. Med. Imaging*, **16**(1):96–107, 1997.
- Chen JS, Pan C, Wu CT and Liu WK. Reproducing kernel particle methods for large deformation analysis of non-linear. *Comput. Methods Appl. Mech. Eng.*, **139**(1-4):195–227, 1996.
- Chen JS, Yoon S, Wang H and Liu WK. An improved reproducing kernel particle method for nearly incompressible finite elasticity. *Comput. Methods Appl. Mech. Eng.*, **181**(1–3):117–145, 2000.
- Chen JS, Han W, You Y and Meng X. A reproducing kernel method with nodal interpolation property. *Int. J. Numer. Methods Eng.*, **56**(7):935–960, 2003.
- Chu YA and Moran B. A computational model for nucleation of solid-solid phase transformations. *Model. Simul. Mater. Sci. Eng.*, **3**:455–471, 1995.
- Cordes LW and Moran B. Treatment of material discontinuity in the element-free Galerkin method. *Comput. Methods Appl. Mech. Eng.*, **139**(1–4):75–89, 1996.
- Daux C, Moes N, Dolbow J, Sukumar N and Belytschko T. Arbitrary branched and intersecting cracks with the extended finite element method. *Int. J. Numer. Methods Eng.*, **48**(12):1741–1760, 2000.
- De S and Bathe KJ. The method of finite spheres. *Comput. Mech.*, **25**(4):329–345, 2000.
- Díez P, Arroyo M and Huerta A. Adaptivity based on error estimation for viscoplastic softening materials. *Mech. Cohesive-Frict. Mater.*, **5**(2):87–112, 2000.

- Dilts G. Moving-least-square-particles-hydrodynamics I: Consistency and stability. *Int. J. Numer. Methods Eng.*, **44**(8):1115–1155, 1999.
- Dolbow J and Belytschko T. Volumetric locking in the element free Galerkin method. *Int. J. Numer. Methods Eng.*, **46**(6):925–942, 1999.
- Dolbow J, Moes N and Belytschko T. Discontinuous enrichment in finite elements with a partition of unity method. *Finite Elem. Anal. and Des.*, **36**(3–4):235–260, 2000.
- Donea J and Huerta A. *Finite element methods for flow problems*. John Wiley & Sons, Chichester, 2003.
- Duarte CA and Oden JT. h - p clouds – an h - p meshless method. *Numer. Methods Partial Differ. Equations*, **12**(6):673–705, 1996.
- Duarte CA and Oden JT. An h - p adaptive method using clouds. *Comput. Methods Appl. Mech. Eng.*, **139**(1-4):237–262, 1996.
- Dyka CT. Addressing tension instability in SPH methods. Technical Report NRL/MR/6384, NRL, 1994.
- Fernández-Méndez S and Huerta A. Coupling finite elements and particles for adaptivity: An application to consistently stabilized convection-diffusion. In Griebel M and Schweitzer MA, editors, *Meshfree methods for partial differential equations*, volume 26 of *Lecture Notes in Computational Science and Engineering*, pages 117–129. Springer-Verlag, Berlin, 2002.
- Fernández-Méndez S and Huerta A. Imposing essential boundary conditions in mesh-free methods. *Comput. Methods Appl. Mech. Eng.*, **193**, 2004.
- Fernández-Méndez S, Díez P and Huerta A. Convergence of finite elements enriched with meshless methods. *Numer. Math.*, **96**(1):43–59, 2003.
- Fleming M, Chu YA, Moran B and Belytschko T. Enriched element-free Galerkin methods for crack tip fields. *Int. J. Numer. Methods Eng.*, **40**(8):1483–1504, 1997.
- Freud J and Stenberg R. On weakly imposed boundary conditions for second order problems. In *Proceeding of the International Conference on Finite Elements in Fluids - New trends and applications, Venezia*, 1995.
- Gingold RA and Monaghan JJ. Smoothed particle hydrodynamics: theory and application to non-spherical stars. *Mon. Notices Royal Astro. Soc.*, **181**:375–389, 1977.
- Girault V and Raviart PA. *Finite element methods for Navier-Stokes equations. Theory and algorithms*. Springer-Verlag, Berlin, 1986.
- Gosz J and Liu WK. Admissible approximations for essential boundary conditions in the reproducing kernel particle method. *Comput. Mech.*, **19**(2):120–135, 1996.
- Gresho PM and Sani RL. *Incompressible flow and the finite element method. Vol. 1: Advection diffusion. Vol. 2: Isothermal laminar flow*. John Wiley & Sons, Chichester, 2000.
- Griebel M and Schweitzer MA. A particle-partition of unity method. Part V: Boundary conditions. In Hildebrandt S and Karcher H, editors, *Geometric Analysis and Nonlinear Partial Differential Equations*, pages 517–540, Berlin, 2002. Springer.
- Günter FC and Liu WK. Implementation of boundary conditions for meshless methods. *Comput. Methods Appl. Mech. Eng.*, **163**(1-4):205–230, 1998.

- Gunzburger MD. *Finite element methods for viscous incompressible flows. A guide to theory, practice, and algorithms.* Academic Press, Boston, MA, 1989.
- Hansbo P and Larson MG. Discontinuous Galerkin methods for incompressible and nearly incompressible elasticity by Nitsche's method. *Comput. Methods Appl. Mech. Engrg.*, **191**(17-18):1895–1908, 2002.
- Hegen D. Element free Galerkin methods in combination with finite element approaches. *Comput. Methods Appl. Mech. Engrg.*, **135**(1-2):143–166, 1996.
- Huerta A and Díez P. Error estimation including pollution assessment for nonlinear finite element analysis. *Comput. Methods Appl. Mech. Engrg.*, **181**(1–3):21–41, 2000.
- Huerta A and Fernández-Méndez S. Enrichment and coupling of the finite element and meshless methods. *Int. J. Numer. Methods Eng.*, **48**(11):1615–1636, 2000.
- Huerta A and Fernández-Méndez S. Locking in the incompressible limit for the element free Galerkin method. *Int. J. Numer. Methods Eng.*, **51**(11):1361–1383, 2001.
- Huerta A, Fernández-Méndez S and Díez P. Enrichissement des interpolations d'éléments finis en utilisant des méthodes de particules. *ESAIM-Math. Model. Numer. Anal.*, **36**(6):1027–1042, 2002.
- Huerta A, Vidal Y and Villon P. Pseudo-divergence-free element free Galerkin method for incompressible fluid flow. *Comput. Methods Appl. Mech. Engrg.*, **193**, 2004.
- Huerta A, Fernández-Méndez S and Liu WK. A comparison of two formulations to blend finite elements and mesh-free methods. *Comput. Methods Appl. Mech. Engrg.*, **193**, 2004.
- Hughes TJR. *The finite element method: linear static and dynamic finite element analysis.* Dover Publications Inc., New York, 2000. Corrected reprint of the 1987 original [Prentice-Hall Inc., Englewood Cliffs, N.J.].
- Johnson GR and Beissel SR. Normalized smoothing functions for SPH impact computations. *Comput. Methods Appl. Mech. Engrg.*, **39**(16):2725–2741, 1996.
- Kansa E and Carlsson R. Improved accuracy of multiquadric interpolation using variable shape parameters. *Computers and Mathematics with applications*, **24**:88–120, 1992.
- Kansa E. A scattered data approximation scheme with application to computational fluid-dynamics-I and II. *Computers and Mathematics with applications*, **19**:127–161, 1990.
- Krongauz Y and Belytschko T. Consistent pseudo-derivatives in meshless methods. *Comput. Methods Appl. Mech. Engrg.*, **146**(1–4):371–386, 1998.
- Krongauz Y and Belytschko T. EFG approximation with discontinuous derivatives. *Int. J. Numer. Methods Eng.*, **41**(7):1215–1233, 1998.
- Krysl P and Belytschko T. Element-free Galerkin method: Convergence of the continuous and discontinuous shape functions. *Comput. Methods Appl. Mech. Engrg.*, **48**(3–4):257–277, 1997.
- Lancaster GM. Surfaces generated by moving least squares methods. *Math. Comput.*, **3**(37):141–158, 1981.
- Li S and Liu WK. Meshfree and particle methods and their applications. *Appl. Mech. Rev.*, **55**(4):1–34, 2002.

- Liszka T and Orkisz J. The finite difference method at arbitrary irregular grids and its application in applied mechanics. *Comput. Struct.*, **11**:83–95, 1980.
- Liu WK, Jun S and Zhang YF. Reproducing kernel particle methods. *Int. J. Numer. Methods Fluids*, **20**(8–9):1081–1106, 1995.
- Liu WK, Jun S, Li S, Adee J and Belytschko T. Reproducing kernel particle methods for structural dynamics. *Int. J. Numer. Methods Eng.*, **38**(10):1655–1679, 1995.
- Liu WK, Belytschko T and Oden JT., editors. Meshless methods. *Comput. Methods Appl. Mech. Eng.*, **139**(1–4):1–440, 1996.
- Liu WK, Chen Y, Jun S, Chen JS, Belytschko T, Pan C, Uras RA and Chang CT. Overview and applications of the reproducing kernel particle methods. *Arch. Comput. Methods Engrg.*, **3**(1):3–80, 1996.
- Liu WK, Li S and Belytschko T. Moving least square reproducing kernel methods Part I: Methodology and convergence. *Comput. Methods Appl. Mech. Eng.*, **143**(1–2):113–154, 1997.
- Liu WK, Uras RA and Chen Y. Enrichment of the finite element method with the reproducing kernel particle method. *J. Appl. Mech., ASME*, **64**:861–870, 1997.
- Lucy L. A numerical approach to the testing of the fission hypothesis. *Astron. J.*, **82**:1013–1024, 1977.
- Melenk JM and Babuška I. The partition of unity finite element method: basic theory and applications. *Comput. Methods Appl. Mech. Eng.*, **139**(1–4):289–314, 1996.
- Moes N, Dolbow J and Belytschko T. A finite element method for crack growth without remeshing. *Int. J. Numer. Methods Eng.*, **46**(1):131–150, 1999.
- Monaghan JJ. Why particle methods work. *SIAM J. Sci. Stat. Comput.*, **3**(3):422–433, 1982.
- Monaghan JJ. An introduction to SPH. *Comput. Phys. Commun.*, **48**(1):89–96, 1988.
- Nayroles B, Touzot G and Villon P. Generating the finite element method: diffuse approximation and diffuse elements. *Comput. Mech.*, **10**(5):307–318, 1992.
- Nitsche J. Über eine variation zur lösung von dirichlet-problemen bei verwendung von teilräumen die keinen randbedingungen unterworfen sind. *Abh. Math. Se. Univ.*, **36**:9–15, 1970.
- Oden and Duarte. *Clouds, cracks and fem's*. 1997. In B.D. Reddy, editor, Recent developments in computational and applied mechanics. A volume in honour of J.B. Martin. Barcelona: CIMNE, pages 302–321.
- Oñate E and Idelsohn S. A mesh-free finite point method for advective-diffusive transport and fluid flow problems. *Comput. Mech.*, **21**(4-5):283–292, 1998.
- Organ D, Fleming M, Terry T and Belytschko T. Continuous meshless approximations for nonconvex bodies by diffraction and transparency. *Comput. Mech.*, **18**(3):225–235, 1996.
- Orkisz J. Meshless finite difference method. i basic approach. In *Proc. of the IACM-Fourth World Congress in Computational Mechanics*, CIMNE, 1998.
- Perrone N and Kao R. A general finite difference method for arbitrary meshes. *Comput. Struct.*, **5**:45–58, 1975.

- Pironneau O. *Finite element methods for fluids*. John Wiley & Sons, Chichester, 1989.
- Quartapelle L. *Numerical solution of the incompressible Navier-Stokes equations*, volume 113 of *International Series of Numerical Mathematics*. Birkhäuser-Verlag, Basel, 1993.
- Quarteroni A and Valli A. *Numerical Approximation of Partial Differential Equations*, volume 23 of *Springer Series in Computational Mathematics*. Springer-Verlag, Berlin, 1994.
- Randles PW and Libersky LD. Smoothed particle hydrodynamics: some recent improvements and applications. *Comput. Methods Appl. Mech. Eng.*, **139**(1–4):375–408, 1996.
- Randles PW and Libersky LD. Normalized SPH with stress points. *Int. J. Numer. Methods Eng.*, **48**(10):1445–1462, 2000.
- Rippa S. An algorithm for selecting a good value for the parameter c in radial basis function interpolation. *Advances in Computational Mechanics*, **11**:193–210, 1999.
- Schweitzer. *A parallel multilevel partition of unity method for elliptic partial differential equations*. Springer, 2003. Lecture Notes in Computational Science and Engineering.
- Sharan M, Kansa E and Gupta S. Application of the multiquadric method for numerical solution of elliptic partial differential equations. *Applied Mathematics and Computations*, **84**:275–302, 1997.
- Sukumar N, Chopp DL, Moes N and Belytschko T. Modeling holes and inclusions by level sets in the extended finite-element method. *Comput. Methods Appl. Mech. Eng.*, **190**(46–47):6183–6200, 2001.
- Suri M. Analytical and computational assessment of locking in the hp finite element method. *Comput. Methods Appl. Mech. Eng.*, **133**(3–4):347–371, 1996.
- Sweegle JW, Hicks DL and Attaway SW. Smoothed particle hydrodynamics stability analysis. *J. Comput. Phys.*, **116**:123–134, 1995.
- Temam R. *Navier-Stokes equations. Theory and numerical analysis*. AMS Chelsea Publishing, Providence, RI, 2001. Corrected reprint of the 1984 edition [North-Holland, Amsterdam, 1984].
- Ventura G, Xu J and Belytschko T. A vector level set method and new discontinuity approximations for crack growth by EFG. *Int. J. Numer. Methods Eng.*, **54**(6):923–944, 2002.
- Vidal Y, Villon P and Huerta A. Locking in the incompressible limit: pseudo-divergence-free element-free Galerkin. *Revue européenne des éléments finis*, **11**(7/8):869–892, 2002.
- Vila JP. On particle weighted methods and smooth particle hydrodynamics. *Math. Models Methods Appl. Sci.*, **9**(2):161–209, 1999.
- Villon P. *Contribution à l'optimisation*. Thèse présentée pour l'obtention du grade de docteur d'état, Université de Technologie de Compiègne, Compiègne, France, 1991.
- Wagner GJ and Liu WK. Application of essential boundary conditions in mesh-free methods: a corrected collocation method. *Int. J. Numer. Methods Eng.*, **47**(8):1367–1379, 2000.
- Wagner GJ and Liu WK. Hierarchical enrichment for bridging scales and mesh-free boundary conditions. *Int. J. Numer. Methods Eng.*, **50**(3):507–524, 2001.

- Wells GN, de Borst R and Sluys LJ. A consistent geometrically non-linear approach for delamination. *Int. J. Numer. Methods Eng.*, **54**(9):1333–1355, 2002.
- Wendland H. Meshless Galerkin methods using radial basis functions. *Math. Comp.*, **68**(228):1521–1531, 1999.
- Wendland H. Local polynomial reproduction and moving least squares approximation. *IMA J. Numer. Anal.*, **21**:285–300, 2001.
- Wu ZM and Schaback R. Local error-estimates for radial basis function interpolation of scattered data. *IMA. J. Numer. Anal.*, **13**(1):13–27, 1993.
- Xiao QZ and Karihaloo BL. Direct evaluation of accurate coefficients of the linea elastic crack tip asymptotic field. *Fatigue Fract. Eng. M.*, **26**(8):719–729, 2003.
- Zhu T and Atluri SN. A modified collocation method and a penalty formulation for enforcing the essential boundary conditions in the element free Galerkin method. *Comput. Mech.*, **21**(3):211–222, 1998.